Barwell J, Conner A, Poyner DR (2011). Extracellular loops 1 and 3 and their associated transmembrane regions of the calcitonin receptor-like receptor are needed for CGRP receptor function. Biochim Biophys Acta 1813: 1906–1916.

Christopoulos A, Christopoulos G, Morfis M, Udawela M, Laburthe M, Couvineau A *et al.* (2003). Novel receptor partners and function of receptor activity-modifying proteins. J Biol Chem 278: 3293–3297.

Chugunov AO, Simms J, Poyner DR, Dehouck Y, Rooman M, Gilis D *et al.* (2010). Evidence that interaction between conserved residues in transmembrane helices 2, 3, and 7 are crucial for human VPAC1 receptor activation. Mol Pharmacol 78: 394–401.

Claus M, Jaeschke H, Kleinau G, Neumann S, Krause G, Paschke R (2005). A hydrophobic cluster in the center of the third extracellular loop is important for thyrotropin receptor signaling. Endocrinology 146: 5197–5203.

Conner AC, Simms J, Barwell J, Wheatley M, Poyner DR (2007a). Ligand binding and activation of the CGRP receptor. Biochem Soc Trans 35 (Pt 4): 729–732.

Conner M, Hawtin SR, Simms J, Wootten D, Lawson Z, Conner AC *et al.* (2007b). Systematic analysis of the entire second extracellular loop of the V(1a) vasopressin receptor: key residues, conserved throughout a G-protein-coupled receptor family, identified. J Biol Chem 282: 17405–17412.

Flahaut M, Rossier BC, Firsov D (2002). Respective roles of calcitonin receptor-like receptor (CRLR) and receptor activity-modifying proteins (RAMP) in cell surface expression of CRLR/RAMP heterodimeric receptors. J Biol Chem 277: 14731–14737.

Gibbons C, Dackor R, Dunworth W, Fritz-Six K, Caron KM (2007). Receptor activity-modifying proteins: RAMPing up adrenomedullin signaling. Mol Endocrinol 21: 783–796.

Hawtin SR, Simms J, Conner M, Lawson Z, Parslow RA, Trim J *et al.* (2006). Charged extracellular residues, conserved throughout a G-protein-coupled receptor family, are required for ligand binding, receptor activation, and cell-surface expression. J Biol Chem 281: 38478–38488.

Hay DL, Howitt SG, Conner AC, Schindler M, Smith DM, Poyner DR (2003). CL/RAMP2 and CL/RAMP3 produce pharmacologically distinct adrenomedullin receptors: a comparison of effects of adrenomedullin22-52, CGRP8-37 and BIBN4096BS. Br J Pharmacol 140: 477–486.

Hay DL, Poyner DR, Sexton PM (2006). GPCR modulation by RAMPs. Pharmacol Ther 109: 173–197.

Ittner LM, Luessi F, Koller D, Born W, Fischer JA, Muff R (2004). Aspartate(69) of the calcitonin-like receptor is required for its functional expression together with receptor-activity-modifying proteins 1 and -2. Biochem Biophys Res Commun 319: 1203–1209.

Kitamura K, Ichiki Y, Tanaka M, Kawamoto M, Emura J, Sakakibara S *et al.* (1994). Immunoreactive adrenomedullin in human plasma. FEBS Lett 341: 288–290.

Klco JM, Nikiforovich GV, Baranski TJ (2006). Genetic analysis of the first and third extracellular loops of the C5a receptor reveals an essential WXFG motif in the first loop. J Biol Chem 281: 12010–12019.

Kleinau G, Jaeschke H, Mueller S, Raaka BM, Neumann S, Paschke R *et al.* (2008). Evidence for cooperative signal triggering at the extracellular loops of the TSH receptor. FASEB J 22: 2798–2808.

Koller D, Born W, Leuthauser K, Fluhmann B, McKinney RA, Fischer JA *et al.* (2002). The extreme N-terminus of the calcitonin-like receptor contributes to the selective interaction with adrenomedullin or calcitonin gene-related peptide. FEBS Lett 531: 464–468.

Koller D, Ittner LM, Muff R, Husmann K, Fischer JA, Born W (2004). Selective inactivation of adrenomedullin over calcitonin gene-related peptide receptor function by the deletion of amino acids 14-20 of the mouse calcitonin-like receptor. J Biol Chem 279: 20387–20391.

Kuwasako K, Shimekake Y, Masuda M, Nakahara K, Yoshida T, Kitaura M *et al.* (2000). Visualization of the calcitonin receptor-like receptor and its receptor activity-modifying proteins during internalization and recycling. J Biol Chem 275: 29602–29609.

Kuwasako K, Kitamura K, Uemura T, Nagoshi Y, Kato J, Eto T (2003). The function of extracellular cysteines in the human adrenomedullin receptor. Hypertens Res 26 (Suppl): S25–S31.

Kuwasako K, Cao YN, Nagoshi Y, Kitamura K, Eto T (2004a). Adrenomedullin receptors: pharmacological features and possible pathophysiological roles. Peptides 25: 2003–2012.

Kuwasako K, Cao YN, Nagoshi Y, Tsuruda T, Kitamura K, Eto T (2004b). Characterization of the human calcitonin gene-related peptide receptor subtypes associated with receptor activity-modifying proteins. Mol Pharmacol 65: 207–213.

Kuwasako K, Cao YN, Chu CP, Iwatsubo S, Eto T, Kitamura K (2006). Functions of the cytoplasmic tails of the human receptor activity-modifying protein components of calcitonin gene-related peptide and adrenomedullin receptors. J Biol Chem 281: 7205–7213.

Kuwasako K, Kitamura K, Nagata S, Kato J (2008). Functions of the extracellular histidine residues of receptor activity-modifying proteins vary within adrenomedullin receptors. Biochem Biophys Res Commun 377: 109–113.

Kuwasako K, Kitamura K, Nagata S, Kato J (2009). Flow cytometric analysis of the calcitonin receptor-like receptor domains responsible for cell-surface translocation of receptor activity-modifying proteins. Biochem Biophys Res Commun 384: 249–254.

Kuwasako K, Kitamura K, Nagata S, Hikosaka T, Kato J (2010). Function of the cytoplasmic tail of human calcitonin receptor-like receptor in complex with receptor activity-modifying protein 2. Biochem Biophys Res Commun 392: 380–385.

Kuwasako K, Kitamura K, Nagata S, Hikosaka T, Kato J (2011a). Structure-function analysis of helix 8 of human calcitonin receptor-like receptor within the adrenomedullin 1 receptor. Peptides 32: 144–149.

Kuwasako K, Kitamura K, Nagata S, Hikosaka T, Takei Y, Kato J (2011b). Shared and separate functions of the RAMP-based adrenomedullin receptors. Peptides 32: 1540–1550.

Lawson Z, Wheatley M (2004). The third extracellular loop of G-protein-coupled receptors: more than just a linker between two important transmembrane helices. Biochem Soc Trans 32 (Pt 6): 1048–1050.

McLatchie LM, Fraser NJ, Main MJ, Wise A, Brown J, Thompson N *et al.* (1998). RAMPs regulate the transport and ligand specificity of the calcitonin-receptor-like receptor. Nature 393: 333–339.

Muff R, Born W, Fischer JA (2003). Adrenomedullin selectivity of calcitonin-like receptor/receptor activity modifying proteins. Hypertens Res 26 (Suppl): S3–S8.

Nielsen SM, Nielsen LZ, Hjorth SA, Perrin MH, Vale WW (2000). Constitutive activation of tethered-peptide/corticotropin-releasing factor receptor chimeras. Proc Natl Acad Sci U S A 97: 10277–10281.

Peeters MC, van Westen GJ, Li Q, Ijzerman AP (2011). Importance of the extracellular loops in G protein-coupled receptors for ligand recognition and receptor activation. Trends Pharmacol Sci 32: 35–42.

Poyner DR, Sexton PM, Marshall I, Smith DM, Quirion R, Born W *et al.* (2002). International Union of Pharmacology. XXXII. The mammalian calcitonin gene-related peptides, adrenomedullin, amylin, and calcitonin receptors. Pharmacol Rev 54: 233–246.

Qi T, Hay DL (2010). Structure–function relationships of the N-terminus of receptor activity-modifying proteins. Br J Pharmacol 159: 1059–1068.

Runge S, Wulff BS, Madsen K, Brauner-Osborne H, Knudsen LB (2003). Different domains of the glucagon and glucagon-like peptide-1 receptors provide the critical determinants of ligand selectivity. Br J Pharmacol 138: 787–794.

Salvatore CA, Mallee JJ, Bell IM, Zartman CB, Williams TM, Koblan KS *et al.* (2006). Identification and pharmacological characterization of domains involved in binding of CGRP receptor antagonists to the calcitonin-like receptor. Biochemistry 45: 1881–1887.

Sexton PM, Poyner DR, Simms J, Christopoulos A, Hay DL (2009). Modulating receptor function through RAMPs: can they represent drug targets in themselves? Drug Discov Today 14: 413–419.

Simpson LM, Wall ID, Blaney FE, Reynolds CA (2011). Modeling GPCR active state conformations: the beta(2)-adrenergic receptor. Proteins 79: 1441–1457.

Siu FY, Stevens RC (2010). RAMP-ing up class-B GPCR ECD structural coverage. Structure 18: 1067–1068.

Standfuss J, Edwards PC, D'Antona A, Fransen M, Xie G, Oprian DD *et al.* (2011). The structural basis of agonist-induced activation in constitutively active rhodopsin. Nature 471: 656–660.

Topiol S, Sabio M (2009). X-ray structure breakthroughs in the GPCR transmembrane region. Biochem Pharmacol 78: 11–20.

Unson CG, Wu CR, Jiang Y, Yoo B, Cheung C, Sakmar TP *et al.* (2002). Roles of specific extracellular domains of the glucagon receptor in ligand binding and signaling. Biochemistry 41: 11795–11803.

Van Rampelbergh J, Juarranz MG, Perret J, Bondue A, Solano RM, Delporte C *et al.* (2000). Characterization of a novel VPAC(1) selective agonist and identification of the receptor domains implicated in the carboxyl-terminal peptide recognition. Br J Pharmacol 130: 819–826.

Walker CS, Conner AC, Poyner DR, Hay DL (2010). Regulation of signal transduction by calcitonin gene-related peptide receptors. Trends Pharmacol Sci 31: 476–483.

Wess J, Han SJ, Kim SK, Jacobson KA, Li JH (2008). Conformational changes involved in G-protein-coupled-receptor activation. Trends Pharmacol Sci 29: 616–625.

Wheatley M, Wootten D, Conner MT, Simms J, Kendrick R, Logan RT *et al.* (2012). Lifting the lid on G-protein-coupled receptors: the role of extracellular loops. Br J Pharmacol 165: 1688–1703.

Zhao MM, Gaivin RJ, Perez DM (1998). The third extracellular loop of the beta2-adrenergic receptor can modulate receptor/G protein affinity. Mol Pharmacol 53: 524–529.

Peptides 32 (2011) 1825–1831

Contents lists available at ScienceDirect

Peptides

journal homepage: www.elsevier.com/locate/peptides

Adrenomedullin production is increased in colorectal adenocarcinomas; its relation to matrix metalloproteinase-9

Tomomi Hikosaka[a], Toshihiro Tsuruda[a,*], Sayaka Nagata[a], Kenji Kuwasako[b], Kazuyo Tsuchiya[c], Shinri Hoshiko[a], Haruhiko Inatsu[a], Kazuo Chijiiwa[c], Kazuo Kitamura[a]

[a] Department of Internal Medicine, Division of Circulation and Body Fluid Regulation, Faculty of Medicine, University of Miyazaki, 5200 Kihara, Kiyotake, Miyazaki 889-1692, Japan
[b] Frontier Science Research Center, University of Miyazaki, Japan
[c] Department of Surgical Oncology and Regulation of Organ Function, Faculty of Medicine, University of Miyazaki, Japan

ARTICLE INFO

Article history:
Received 15 February 2011
Received in revised form 16 July 2011
Accepted 18 July 2011
Available online 3 August 2011

Keywords:
Adrenomedullin
AM2/IMD
MMP-9
VEGF
Metastasis
Stroma

ABSTRACT

Adrenomedullin (AM) is highly expressed in various cancer cell lines, suggesting a possible association with cancer growth. In the present study, we examined the expression and/or concentration of AM, its related peptide, adrenomedullin2/intermedin (AM2/IMD) and their receptors in human colorectal cancer and the surrounding normal tissue. In addition, we assessed the correlation between the expression of AM and AM2/IMD with that of vascular endothelial growth factor (VEGF)-A and matrix metalloproteinase (MMP)-9. Using a specific immunoradiometric assay, we found that AM concentrations were 2–11-fold higher in colorectal cancer tissues than in the surrounding normal tissues. Moreover, real-time quantitative RT-PCR showed that the expression levels of preproAM (+548%), preproAM2/IMD (+2674%), calcitonin receptor-like receptor (CLR) (+518%), receptor activity modifying protein (RAMP)2 (+281%), RAMP3 (+178%), VEGF-A (+277%) and MMP-9 (+864%) mRNAs were significantly higher in cancer tissues than in the surrounding normal tissues, and there was a positive correlation between the gene expressions of MMP-9 and preproAM ($r = 0.352$; $p = 0.005$), but not with preproAM2/IMD ($r = 0.041$, $p = 0.406$). Both AM and AM2/IMD immunoreactivity were detected mainly within cancer cells, whereas MMP-9 immunoreactivity was mostly seen in the surrounding stroma. These findings suggest that AM produced in colorectal tumors acts in concert with MMP-9 in the stroma to contribute to the pathogenesis of colorectal cancer.

1. Introduction

Colorectal cancer is the fourth most common cause of cancer death, worldwide [10]. It proliferates locally and metastasizes to liver, lung, bone and/or brain, and often recurs after surgical resection. Invasion and metastasis are multistep processes that require sequential interactions between the cancer cells and stromal components, such as the extracellular matrix [12] and micro-neovessels [35]. Matrix metalloproteinases (MMPs) and vascular endothelial growth factor (VEGF) are key factors that facilitate invasion and metastasis, respectively by degrading extracellular matrix [35] and promoting angiogenesis [8,15] for solid tumor growth.

Adrenomedullin (AM) is a piuripotent bioactive peptide initially isolated from human pheochromocytoma [21]. Since its isolation, AM has been shown to be widely distributed among various organs and tissues, including the human digestive system [22,26], and to be involved a variety of physiological functions, such as vasodilatation, hormone secretion, neurotransmission, embryogenesis, wound healing and immunoregulation [2]. Adrenomedullin2/intermedin (AM2/IMD) was identified as an AM-related peptide by genomic searching [34,36]. AM2/IMD possesses not only a structural similarity to AM such as a ring structure and an amidated C terminus, but also a functional analogy to exert vasodilation and anti-oxidative stress [14]. The functions of AM are mediated through specific receptors comprising calcitonin receptor-like receptor (CLR) and a receptor activity-modifying protein (RAMP); when co-expressed with RAMP2 or RAMP3, CLR functions as a specific AM receptor [23]. Meanwhile, AM2/IMD binds non-selectively to three types of CLR/RAMP complexes: CLR/RAMP1, CLR/RAMP2 and CLR/RAMP3 [23]. AM and its receptors are highly expressed in some tumors and cancer cell lines, which suggests that AM may participate in tumor progression through its potent mitogenic, angiogenic and anti-apoptotic properties [1,13,29]. However, its site-specific expression profile and its concentration in human colorectal cancers and the surrounding normal tissue have not been fully explored. Therefore, our aims in the present study were to measure the expression and/or concentration of AM and its receptors in both cancerous and normal colorectal tissue in humans, and to correlate AM levels

* Corresponding author. Tel.: +81 985 85 0872; fax: +81 985 85 6596.
E-mail address: ttsuruda@med.miyazaki-u.ac.jp (T. Tsuruda).

0196-9781/$ – see front matter © 2011 Elsevier Inc. All rights reserved.
doi:10.1016/j.peptides.2011.07.012

Table 1
Sequence of the primers and probes.

Gene	Primer/probe sequences	Product size (bp)
AM	S: 5′-TGCCCAGACCCTTATTCGG-3′ AS: 5′-CCGGAGGCCCTGGAAGT-3′ Probe: 5′-AGTCAAGCGCTACCGCCAGAGCA-3′	130
AM2/IMD	Applied Biosystems Gene Expression Assays (ID;Hs00363866_m1)	
CLR	S: 5′-CTGTACATGAAAGCTGTGAGAGCTACT-3′ AS: 5′-TGGAAGTGCATAAGGATGTGCATGATG-3′ Probe: 5′-TCCATGGCGACCTGAAGGAAAGATTGCAGA-3′	140
RAMP2	S: 5′-GCAGAGAGGATCATCTTTGAGACTC-3′ AS: 5′-CCTCCATACTACAAGAGTGATGAGGAAG-3′ Probe: 5′-TGCTCCCTGGTGCAGCCCACCTCTTCTGAC-3′	156
RAMP3	S: 5′-CCGAGTTCATCGTGTACTATGAGAG-3′ AS: 5′-CTGTGGATGCCGGTGATGAAGC-3′ Probe: 5′-AGGCCAATGTCGTGGGCTACTGGCCCA-3′	115
VEGF-A	S: 5′-GTGTGAGTGGTTGACCTTCCTC-3′ AS: 5′-CCGTATATAAAACACTTTCTCTTTTCTCTG-3′ Probe: 5′-CCTGGTCCTTCCCTTCCCTTCCCGA-3′	125
MMP-9	S: 5′-CCCTGGAGACCTGAGAACCA-3′ AS: 5′-AACCATAGCGGTACAGGTATTCCT-3′ Probe: 5′-TCTCACCGACAGGCAGCTGGCA-3′	78
β-actin	S: 5′-AGCCTCGCCTTTGCCGA-3′ AS: 5′-CTGGTGCCTGGGGCG-3′ Probe: 5′-CCGCCGCCCGTCCACACCCGCC-3′	174

S, sense strand; AS, antisense strand.

with clinical variables and the synthesis of invasive and metastatic factor, VEGF-A and MMP-9. We also discussed the expression of AM2/IMD in the disorder.

2. Materials and methods

2.1. Tissue collection

Colorectal specimens were obtained from 23 Japanese patients with colorectal cancer (8 colon cancer and 15 rectal cancer) who underwent surgical resections at Miyazaki University Hospital between June 2007 and March 2009. The histological stages were determined according to Japanese General Rules for Clinical and Pathological Studies on Cancer of the Colon, Rectum and Anus, The 7th Edition. The specimens (0.2–1.0 g) included both cancerous tissue and normal-appearing colorectal tissue from the surrounding area. All specimens were immediately stored in liquid nitrogen until used for real-time quantitative PCR, immunoradiometric assays (IRMAs) and histological analysis. Written informed consent was obtained from all patients, and the study protocol was approved by the institutional review board (No. 519).

2.2. IRMA

The mature form of AM was measured using an AM mature IRMA kit (Shionogi & Co., Ltd., Osaka, Japan) [30]. Tissue samples boiled in 1.0 mol/L acetic acid were homogenized and centrifuged at 12,000 rpm for 20 min at 4 °C, after which the supernatants were stored at −30 °C until assayed.

2.3. Reverse-phase high performance liquid chromatography (RP-HPLC)

To characterize the molecular forms of immunoreactive AM in human colorectal tissues, collected samples (1.0 g) of cancer tissue and the surrounding normal tissue in one patient were immediately boiled for 10 min and then acidified by the addition of acetic acid to a final concentration of 1.0 mol/L to inactivate proteases. The samples were then homogenized and centrifuged at 12,000 rpm for 20 min, after which the supernatants were applied to Sep-Pak C18 cartridges (Nihon Waters K.K.). The resultant extracts were analyzed by RP-HPLC with a TSK ODS 120A column (4.6 × 150 mm; Tosoh) using a linear gradient from solvent A (H_2O–acetonitrile (CH_3CN)–100 mL/L trifluoroacetic acid (TFA, 90:10:1, by volume)) to solvent B (H_2O–acetonitrile–100 mL/L TFA (40:60:1, by volume)) at a flow rate 1 mL/min for 60 min. The immunoreactive AM in each fraction was measured using an IRMA [30] twice, and identical results were obtained. Synthetic human AM peptide was purchased from PEPTIDE INSTITUTE, INC. Osaka, Japan.

2.4. Real-time quantitative RT-PCR

Real-time quantitative RT-PCR was performed using TaqMan probes to quantify the mRNA levels of AM, AM2/IMD, CLR, RAMP2, RAMP3, VEGF-A, MMP-9 and β-actin. The primers and probes used in this study are listed in Table 1. To quantify the mRNA, standard curves were drawn using diluted cDNA made by human colon tissue. After extracting the total RNA using TRIzol (Life Technologies, Ltd.), 2-μg aliquots were used to synthesize cDNA as previously described [28]. Quantitative RT-PCR analysis was carried out using an Applied Biosystems Prism 7300 Sequence Detector. The PCR protocol entailed a starting cycle of 95 °C for 10 min, followed by 40 cycles of 95 °C for 15 s and 60 °C for 1 min. The PCR products were electrophoresed and found to be of the expected molecular sizes, and β-actin mRNA was used as an internal normalization standard.

2.5. Immunohistochemical staining

Immunohistochemical staining was conducted with samples from all 23 patients after preparation of serial sections. Tissue sections (4 μm) that had been fixed in 10% formalin and embedded in paraffin were deparaffinized, hydrated in 0.01 mol/L phosphate-buffered saline (PBS), and incubated in 3% H_2O_2 in PBS for 20 min at room temperature to block endogenous peroxidase activity. For the detection of MMP-9 and AM2/IMD, prior antigen retrieval was performed by autoclaving the specimens at 121 °C for 15 min in citrate buffer (pH 6.0). The sections were then incubated with a mouse monoclonal antibody against human $AM_{[12-25]}$ (1:500 dilu-

Table 2
Patient characteristics.

Patient characteristics	Numbers
Patients	23
Median age (years) [range]	72 [35–91]
Male/female	15/8
Primary site	
Cecum/A/T/D/S/rectum	1/3/2/0/2/15
Histological stage[a]	
I/II/IIIa/IIIb/IV	1/8/5/4/5
Histological type[a] (all adenocarcinoma, partially overlap)	
tub1/tub2/muc/pap/sig	4/16/3/1/1
Liver/lung metastasis	4/1
Median longest diameter of tumor (mm) [range]	60 [25–122]

Abbreviations: A, ascending colon; T, transverse colon; D, descending colon; S, sigmoid colon; tub1, well differentiated type; tub2, moderately differentiated type; muc, mucinous type; pap, papillary type; sig, signet ring cell type.

[a] Japanese General Rules for Clinical and Pathological Studies on Cancer of the Colon, Rectum and Anus, The 7th edition.

tion; [26,30]) or a rabbit polyclonal antibody against human MMP-9 (1:50 dilution; #3852, Cell Signaling Technology, Inc.) and human $AM2/IMD_{[35-47]}$ (1:4000 dilution, originally made by Dr. Kitamura) for 24 h at 4 °C, followed by incubation for 30 min at room temperature with horseradish peroxidase-labeled polymer conjugated with a secondary antibody (Dako Envision+ System). The immunoreactivity was visualized using 3,3′-diaminobenzidine (Dako), and the sections were counterstained with Mayer's hematoxylin. The positive ratio of AM and MMP-9 immunostaining were analyzed by randomly selected 10 fields in 23 serial sections, and calculated as the percentage of the traced positive field, respectively.

2.6. Statistical analysis

Statistical analysis was carried out using GraphPad Prism 5 (MDF Co., Ltd.). Data are expressed as means ± standard deviation. The Wilcoxon matched-pair signed rank test was used to assess the association between two categorical variables. The Spearman rank correlation test was applied for the comparison of correlations among multiple groups. Difference between variables in clinical stage or type was analyzed by Kruskal–Wallis test. Values of $p < 0.05$ were considered significant.

3. Results

3.1. Patient characteristics

Table 2 shows the characteristics of the patients enrolled in this study. They included 15 males and 8 females, ranging in age from 35 to 91 years (median, 72 years). The primary site was the rectum by 65% of cases, and the histological characteristics varied widely. Among the five patients with stage IV disease, four exhibited liver metastasis and one exhibited lung metastasis.

3.2. Concentration and molecular form of AM in colorectal tumors and surrounding normal tissues

Fig. 1A shows that the concentration of AM was significantly ($p < 0.001$) higher in cancerous tissues (2.3 ± 1.0 pmol/g wet tissue) than in macroscopically normal colorectal tissue (0.7 ± 0.4 pmol/g wet tissue). On reverse phase HPLC, the AM immunoreactivity in both the cancerous tissue and surrounding normal tissue in a patient had one major peak, the elution position of which was identical to that of authentic human $AM_{[1-52]}$ (Fig. 1B).

3.3. Expression of preproAM, preproAM2/IMD, CLR, RAMP2, RAMP3, VEGF-A and MMP-9 mRNAs in colorectal tumors and surrounding normal tissues

Fig. 2 shows that the relative expression levels of the preproAM (A; +548%; $p < 0.0001$), preproAM2/IMD (B; +2674%; $p < 0.0001$), CLR (C; +518%; $p < 0.0001$), RAMP2 (D; +281%; $p < 0.0001$), RAMP3 (E; +178%; $p < 0.005$), VEGF-A (F; +277%; $p < 0.001$) and MMP-9 (G; +864%; $p < 0.0001$) mRNAs were significantly higher in cancerous tissues (Ca) than in the surrounding normal colorectal tissues (N).

3.4. Correlation between the expression of preproAM or preproAM2/IMD and VEGF-A or MMP-9 in colorectal tumors and surrounding normal tissues

The ratios of expression levels of VEGF-A mRNA in the cancerous and surrounding normal tissues (Ca/N) correlate the Ca/N ratios neither for preproAM mRNA ($r = 0.080$; $p = 0.213$, Fig. 3A) nor for preproAM2/IMD mRNA ($r = 0.042$; $p = 0.403$, Fig. 3B). On the other hand, the Ca/N ratios for MMP-9 mRNA did correlated significantly with those for preproAM mRNA ($r = 0.352$; $p = 0.005$, Fig. 3C), but not for preproAM2/IMD mRNA ($r = 0.041$, $p = 0.406$, Fig. 3D).

3.5. Localization of AM, AM2/IMD and MMP-9 immunoreactivity in colorectal tumors and surrounding normal tissues

In normal colorectal tissue, AM immunoreactivity was detected in endothelium, surface epithelium and some stromal cells (Fig. 4A and C). MMP-9 immunoreactivity was faintly detected in some stromal cells (Fig. 4B and D). In cancer tissue, strong AM immunoreactivity was distributed mainly in the cytoplasm of cancer cells and in some fibroblast-like stromal cells (Fig. 4E). Moreover, MMP-9

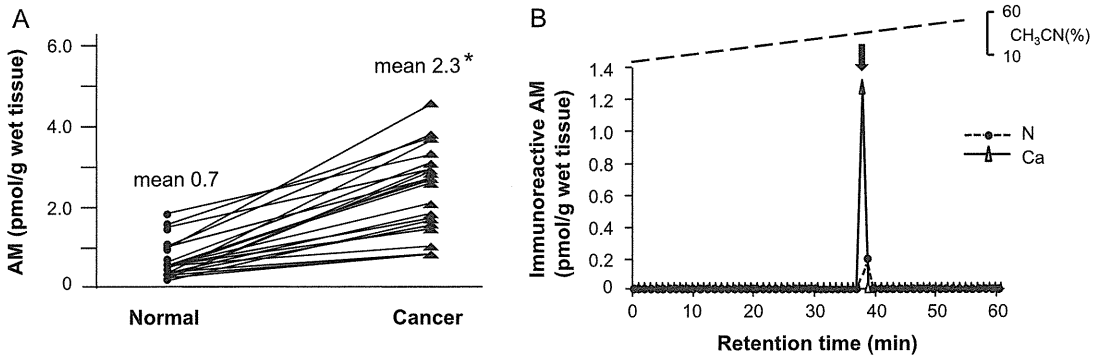

Fig. 1. (A) Concentration of immunoreactive AM in normal and cancerous colorectal tissues from 23 patients. Lines connect symbols indicating the AM concentrations in normal and cancerous tissue from each patient ($n = 23$). The absolute means are also shown in the figure. *$p < 0.001$. (B) RP-HPLC analysis of immunoreactive AM in normal and cancerous tissues from one patient. The arrow indicates the elution position of authentic human $AM_{[1-52]}$. N, Normal; Ca, Cancer tissue.

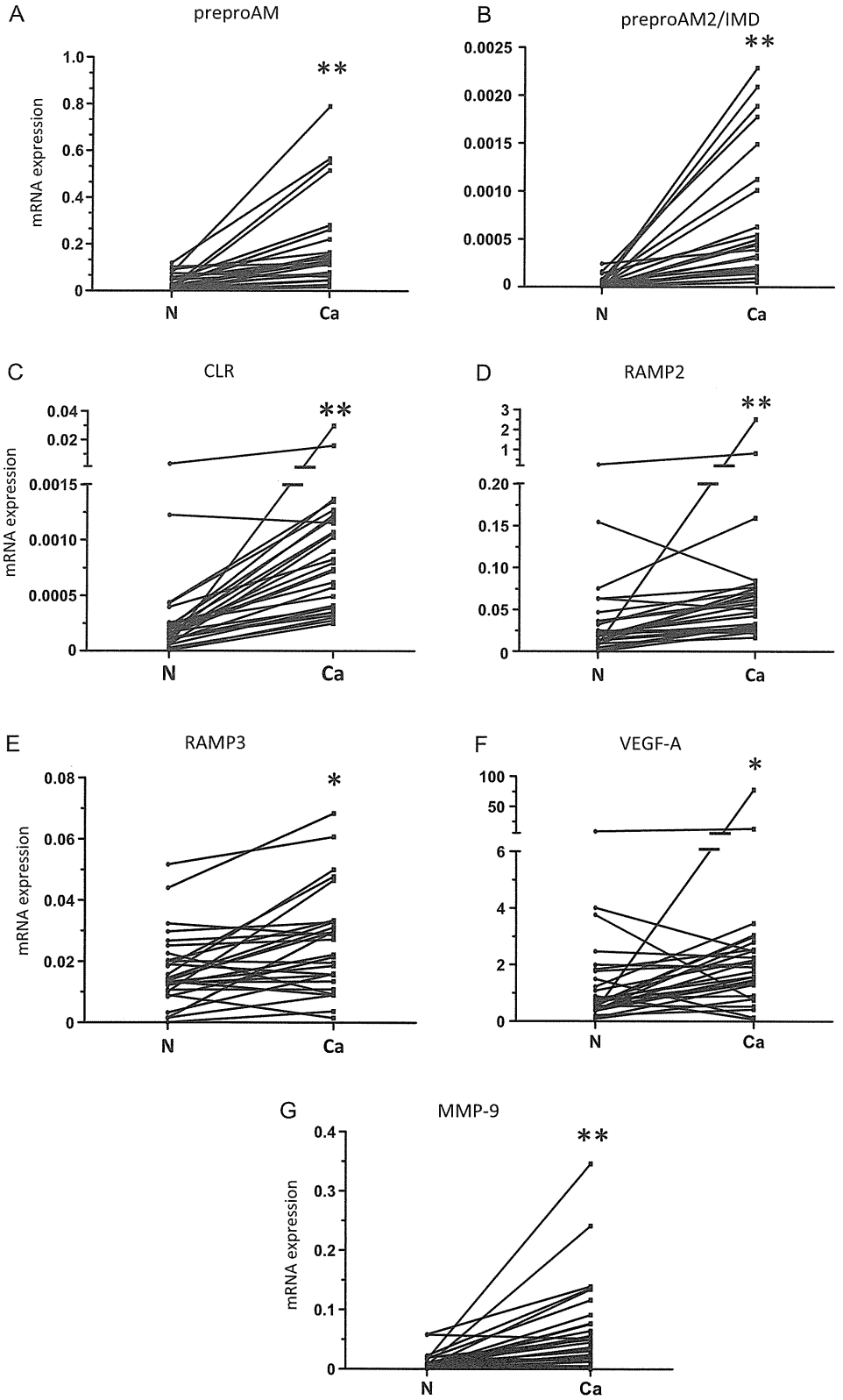

Fig. 2. Expression of preproAM (A), preproAM2/IMD (B), CLR (C), RAMP2 (D), RAMP3 (E), VEGF-A (F) and MMP-9 (G) mRNAs in normal (N) and cancerous tissues (Ca). β-actin served as an internal normalization standard. Lines connect symbols indicating the mRNA expression in the normal and cancerous tissue from each patient ($n = 23$). The *Y*-axes in C, D and F are separated into two segments to make details of the data visible. $^{*}p < 0.001$, $^{**}p < 0.0001$.

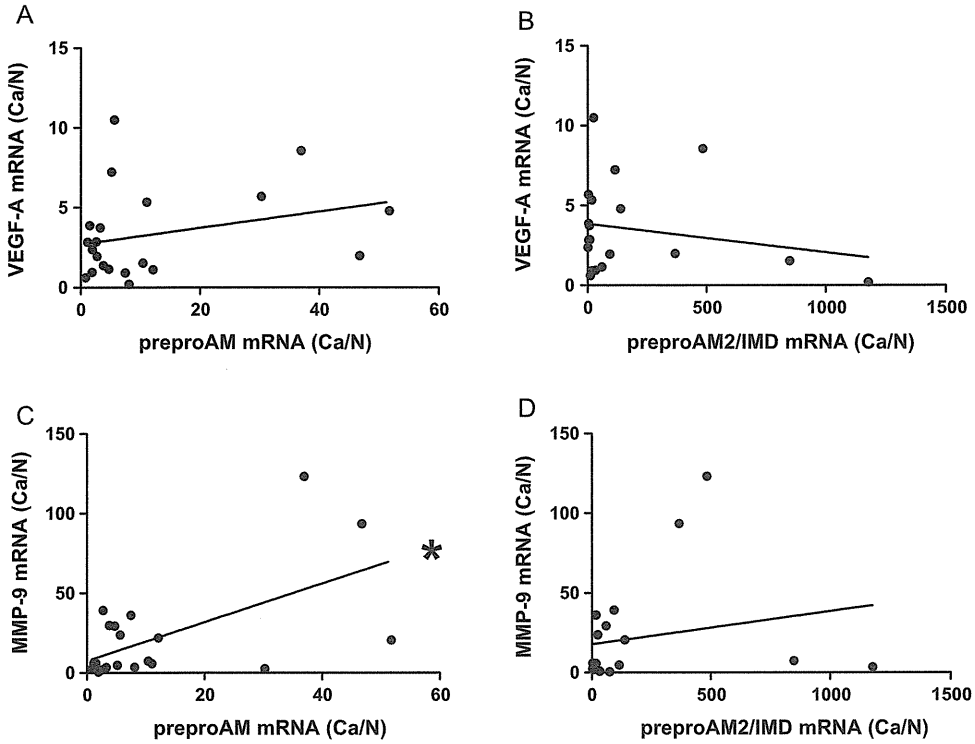

Fig. 3. (A and B) Correlation between the expression ratios of VEGF-A and preproAM mRNAs (A, $r = 0.080$, $p = 0.213$) or preproAM2/IMD mRNAs (B, $r = 0.042$, $p = 0.403$) in the cancerous and surrounding normal colorectal tissues (Ca/N) from each patient. (C and D) Correlation between the expression ratios of MMP-9 and preproAM mRNAs (C, $r = 0.352$, $p = 0.005$) or preproAM2/IMD mRNAs (D, $r = 0.041$, $p = 0.406$) in the cancerous and surrounding normal colorectal tissues (Ca/N) from each patient. $^*p < 0.01$.

immunoreactivity was intensely present in the stroma of cancer tissue (Fig. 4F). MMP-9-positive cells were often found surrounding the AM-positive cells in the serial section, and the positive ratios of AM and MMP-9 in the tissue sections were 14.4% and 11.1% in the fields of cancer tissue specimens, respectively. AM2/IMD immunoreactivity was scattery found in stroma of normal colorectal tissue (Fig. 4G), while it was intensely detected in cancer cells (Fig. 4H).

4. Discussion

AM and its specific receptors, CLR/RAMP2 and CLR/RAMP3, are expressed in various cancer cell lines and in cancers of the pancreas, lung, kidney, breast, ovary and prostate [3,7,27,33]. In addition, AM has been shown to promote tumor growth by stimulating cell proliferation and angiogenesis and inhibiting apoptosis [9,13,18] under hypoxic conditions that lead to AM activation [20]. Conversely, neutralizing AM activity using a specific antibody reduces the growth in glioblastoma cells [31] and pancreatic [18] and colorectal adenocarcinoma cells [19]. However, there have been few studies examining the site-specific expression profiles of the genes encoding AM and its receptors, or the levels of the translated peptides in patients with colorectal cancer. In the present study, we found that colorectal cancers exhibited higher levels of AM synthesis than the surrounding normal tissues.

Most colonic cancer tissue contains substantial amounts of MMP-9 [6] and VEGF [5], co-activation of which is thought to facilitate invasion and metastasis [16]. Consistent with that idea, we found that cancerous colorectal tissue contains significantly higher levels of both MMP-9 and VEGF-A than the surrounding normal tissues. However, the precise mechanism of AM on angiogenesis is unclear; Iimuro et al. [17] reported that AM enhances angiogenesis mediated by VEGF, whereas Fernandes-Sauze et al. [11] found that the proangiogenic action of AM is VEGF-independent. In the present study, expression of preproAM mRNA did not correlate with VEGF mRNA expression. On the other hand, magnitude of MMP-9 mRNA significantly correlated with that of preproAM mRNA. More interestingly, AM appeared to localize specifically in cancer cells, while MMP-9 localized in surrounding stromal cells. AM modulates the production of MMP-2 in rheumatoid synovial fibroblasts [24], aortic adventitial fibroblasts [37], and hepatic stellate cells [38]. On the other hand, amino-acid sequence of AM is reported to be cleaved by MMP-2, but not by MMP-9 [25]. Our finding implicates a cross-talk between cancer cells and the microenvironment during tumor progression through activation of AM and MMP-9. We also found that AM-related peptide, AM2/IMD was highly expressed in colorectal cancer tissue as well. Importantly, the percent increase of AM2/IMD synthesis in cancer tissues to the surrounding normal tissues was greater than AM. The pathological role of AM2/IMD remains to be elucidated in cancer development. AM2/IMD mRNA is up-regulated along with AM under hypoxic conditions [4]. However, we did not find any relationship between preproAM2/IMD mRNA and VEGF-A or MMP-9 synthesis in the present study, implicating a distinct role of these peptides in the tumor progression. Further experiments will be necessary to precisely characterize the pathophysiological roles of AM and AM2/IMD in colorectal cancer development.

Although it has been suggested that plasma AM level appears to be predictive in tumor progression [32], our data are consistent with a report by Buyukberber et al. [3] that AM expression did not associate with any clinical variables, such as histological type ($\chi^2 = 1.77$, $p = 0.78$) or stage ($\chi^2 = 3.17$, $p = 0.53$). We speculate that AM does not directly contribute to tumor progression, but that they more likely have mixed biological effects supporting colon cancer survival in association with matrix degradation.

In summary, this study highlights that expressions of AM and AM2/IMD are increased in human colorectal cancer coinciding with

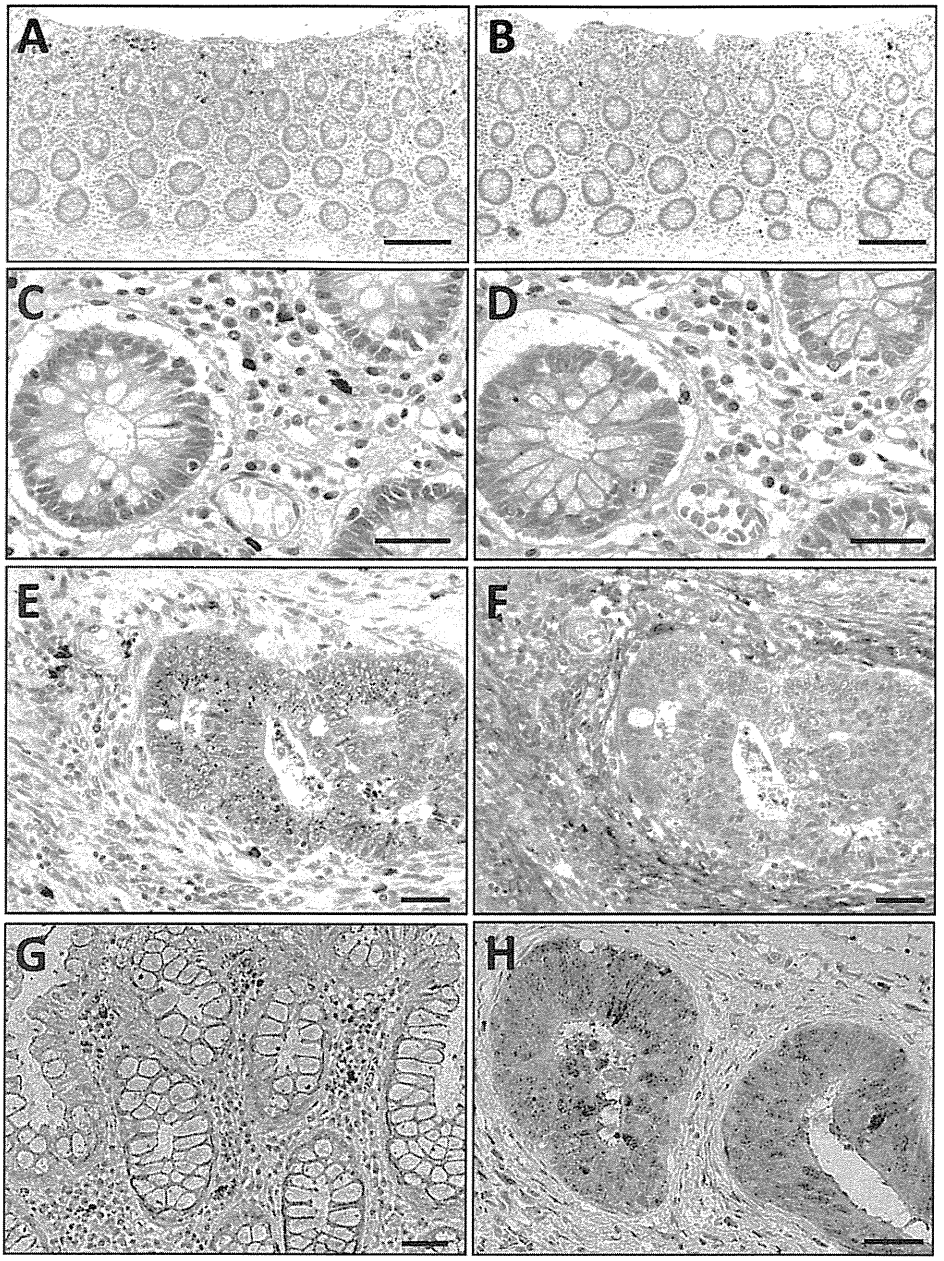

Fig. 4. Representative immunohistochemical staining of AM, MMP-9 and AM2/IMD in sections of human colorectal tissue. (A–D) Immunostaining of AM (A and C) and MMP-9 (B and D) in normal colorectal tissue collected from a patient with colorectal cancer. (E and F) Immunostaining of AM (E) and MMP-9 (F) in moderately differentiated adenocarcinoma tissue. (G and H) Immunostaining of AM2/IMD in normal colorectal tissue (G) and moderately differentiated adenocarcinoma tissue (H). Bars: A, B = 20 μm; C–H = 5 μm.

MMP-9 and VEGF-A in surrounding stroma, suggesting a possible involvement in tumor survival/progression.

Conflicts of interest

None declared.

Acknowledgments

We thank Ms. Ritsuko Sotomura, Ms. Mariko Tokashiki and Ms. Yoko Sekita for their special technical assistance. This study was supported in part by Grants-in-aid for Scientific Research from the Ministry of Health, Labour and Welfare in Japan: H21TR005 (K.K.), and Grants-in-aid from the Mitsubishi Pharma Research Foundation (T.T.).

References

[1] Abasolo I, Montuenga LM, Calvo A. Adrenomedullin prevents apoptosis in prostate cancer cells. Regul Pept 2006;133:115–22.
[2] Beltowski J, Jamroz A. Adrenomedullin—what do we know 10 years since its discovery? Pol J Pharmacol 2004;56:5–27.
[3] Buyukberber S, Sari I, Camci C, Buyukberber NM, Sevinc A, Turk HM. Adrenomedullin expression does not correlate with survival in lung cancer. Med Oncol 2007;24:245–9.
[4] Copple BL, Bustamante JJ, Welch TP, Kim ND, Moon JO. Hypoxia-inducible factor-dependent production of profibrotic mediators by hypoxic hepatocytes. Liver Int 2009;29:1010–21.

[5] Cristi E, Perrone G, Toscano G, Verzi A, Nori S, Santini D, et al. Tumour proliferation, angiogenesis, and ploidy status in human colon cancer. J Clin Pathol 2005;58:1170–4.
[6] Curran S, Dundas SR, Buxton J, Leeman MF, Ramsay R, Murray GI. Matrix metalloproteinase/tissue inhibitors of matrix metalloproteinase phenotype identifies poor prognosis colorectal cancers. Clin Cancer Res 2004;10:8229–34.
[7] Cuttitta F, Pio R, Garayoa M, Zudaire E, Julian M, Elsasser TH, et al. Adrenomedullin functions as an important tumor survival factor in human carcinogenesis. Microsc Res Tech 2002;57:110–9.
[8] Des Guetz G, Uzzan B, Nicolas P, Cucherat M, Morere JF, Benamouzig R, et al. Microvessel density and VEGF expression are prognostic factors in colorectal cancer. Meta-analysis of the literature. Br J Cancer 2006;94:1823–32.
[9] Deville JL, Bartoli C, Berenguer C, Fernandez-Sauze S, Kaafarani I, Delfino C, et al. Expression and role of adrenomedullin in renal tumors and value of its mRNA levels as prognostic factor in clear-cell renal carcinoma. Int J Cancer 2009;125:2307–15.
[10] Ferlay J, Shin HR, Bray F, Forman D, Mathers C, Parkin DM. Estimates of worldwide burden of cancer in 2008: GLOBOCAN 2008. Int J Cancer 2010.
[11] Fernandez-Sauze S, Delfino C, Mabrouk K, Dussert C, Chinot O, Martin PM, et al. Effects of adrenomedullin on endothelial cells in the multistep process of angiogenesis: involvement of CRLR/RAMP2 and CRLR/RAMP3 receptors. Int J Cancer 2004;108:797–804.
[12] Fox SB, Gatter KC, Bicknell R, Going JJ, Stanton P, Cooke TG, et al. Relationship of endothelial cell proliferation to tumor vascularity in human breast cancer. Cancer Res 1993;53:4161–3.
[13] Fritz-Six KL, Dunworth WP, Li M, Caron KM. Adrenomedullin signaling is necessary for murine lymphatic vascular development. J Clin Invest 2008;118:40–50.
[14] Hashimoto H, Kitamura K, Kawasaki M, Saito T, Suzuki H, Otsubo H, et al. Adrenomedullin 2/intermedin-like immunoreactivity in the hypothalamus and brainstem of rats. Auton Neurosci 2008;139:46–54.
[15] Hawinkels LJ, Zuidwijk K, Verspaget HW, de Jonge-Muller ES, van Duijn W, Ferreira V, et al. VEGF release by MMP-9 mediated heparan sulphate cleavage induces colorectal cancer angiogenesis. Eur J Cancer 2008;44:1904–13.
[16] Heslin MJ, Yan J, Johnson MR, Weiss H, Diasio RB, Urist MM. Role of matrix metalloproteinases in colorectal carcinogenesis. Ann Surg 2001;233:786–92.
[17] Iimuro S, Shindo T, Moriyama N, Amaki T, Niu P, Takeda N, et al. Angiogenic effects of adrenomedullin in ischemia and tumor growth. Circ Res 2004;95:415–23.
[18] Ishikawa T, Chen J, Wang J, Okada F, Sugiyama T, Kobayashi T, et al. Adrenomedullin antagonist suppresses in vivo growth of human pancreatic cancer cells in SCID mice by suppressing angiogenesis. Oncogene 2003;22:1238–42.
[19] Kaafarani I, Fernandez-Sauze S, Berenguer C, Chinot O, Delfino C, Dussert C, et al. Targeting adrenomedullin receptors with systemic delivery of neutralizing antibodies inhibits tumor angiogenesis and suppresses growth of human tumor xenografts in mice. FASEB J 2009;23:3424–35.
[20] Keleg S, Kayed H, Jiang X, Penzel R, Giese T, Buchler MW, et al. Adrenomedullin is induced by hypoxia and enhances pancreatic cancer cell invasion. Int J Cancer 2007;121:21–32.
[21] Kitamura K, Kangawa K, Kawamoto M, Ichiki Y, Nakamura S, Matsuo H, et al. Adrenomedullin: a novel hypotensive peptide isolated from human pheochromocytoma. Biochem Biophys Res Commun 1993;192:553–60.
[22] Kitani M, Sakata J, Asada Y, Kitamura K, Eto T. Distribution and expression of adrenomedullin in human gastrointestinal tissue. Ann Clin Biochem 1998;35(Pt 5):643–8.
[23] Kuwasako K, Kitamura K, Nagata S, Hikosaka T, Takei Y, Kato J. Share and separate functions of the RAMP-based adrenomedullin receptors. Peptides 2011.
[24] Lee EG, Lee SI, Chae HJ, Park SJ, Lee YC, Yoo WH. Adrenomedullin inhibits IL-1β-induced rheumatoid synovial fibroblast proliferation and MMPs, COX-2 and PGE2 production. Inflammation 2010.
[25] Martinez A, Oh HR, Unsworth EJ, Bregonzio C, Saavedra JM, Stetler-Stevenson WG, et al. Matrix metalloproteinase-2 cleavage of adrenomedullin produces a vasoconstrictor out of a vasodilator. Biochem J 2004;383:413–8.
[26] Marutsuka K, Hatakeyama K, Sato Y, Yamashita A, Sumiyoshi A, Asada Y. Immunohistological localization and possible functions of adrenomedullin. Hypertens Res 2003;26(Suppl):S33–40.
[27] Miller MJ, Martinez A, Unsworth EJ, Thiele CJ, Moody TW, Elsasser T, et al. Adrenomedullin expression in human tumor cell lines. Its potential role as an autocrine growth factor. J Biol Chem 1996;271:23345–51.
[28] Nagoshi Y, Kuwasako K, Ito K, Uemura T, Kato J, Kitamura K, et al. The calcitonin receptor-like receptor/receptor activity-modifying protein 1 heterodimer can function as a calcitonin gene-related peptide-(8–37)-sensitive adrenomedullin receptor. Eur J Pharmacol 2002;450:237–43.
[29] Nikitenko LL, Fox SB, Kehoe S, Rees MC, Bicknell R. Adrenomedullin and tumour angiogenesis. Br J Cancer 2006;94:1–7.
[30] Ohta H, Tsuji T, Asai S, Sasakura K, Teraoka H, Kitamura K, et al. One-step direct assay for mature-type adrenomedullin with monoclonal antibodies. Clin Chem 1999;45:244–51.
[31] Ouafik L, Sauze S, Boudouresque F, Chinot O, Delfino C, Fina F, et al. Neutralization of adrenomedullin inhibits the growth of human glioblastoma cell lines in vitro and suppresses tumor xenograft growth in vivo. Am J Pathol 2002;160:1279–92.
[32] Pavel ME, Hoppe S, Papadopoulos T, Linder V, Mohr B, Hahn EG, et al. Adrenomedullin is a novel marker of tumor progression in neuroendocrine carcinomas. Horm Metab Res 2006;38:112–8.
[33] Ramachandran V, Arumugam T, Hwang RF, Greenson JK, Simeone DM, Logsdon CD. Adrenomedullin is expressed in pancreatic cancer and stimulates cell proliferation and invasion in an autocrine manner via the adrenomedullin receptor, ADMR. Cancer Res 2007;67:2666–75.
[34] Roh J, Chang CL, Bhalla A, Klein C, Hsu SY. Intermedin is a calcitonin/calcitonin gene-related peptide family peptide acting through the calcitonin receptor-like receptor/receptor activity-modifying protein receptor complexes. J Biol Chem 2004;279:7264–74.
[35] Stetler-Stevenson WG, Liotta LA, Kleiner Jr DE. Extracellular matrix 6: role of matrix metalloproteinases in tumor invasion and metastasis. FASEB J 1993;7:1434–41.
[36] Takei Y, Inoue K, Ogoshi M, Kawahara T, Bannai H, Miyano S. Identification of novel adrenomedullin in mammals: a potent cardiovascular and renal regulator. FEBS Lett 2004;556:53–8.
[37] Tsuruda T, Kato J, Cao YN, Hatakeyama K, Masuyama H, Imamura T, et al. Adrenomedullin induces matrix metalloproteinase-2 activity in rat aortic adventitial fibroblasts. Biochem Biophys Res Commun 2004;325:80–4.
[38] Wang Y, Zhang JS, Qian J, Huang GC, Chen Q. Adrenomedullin regulates expressions of transforming growth factor-β1 and β1-induced matrix metalloproteinase-2 in hepatic stellate cells. Int J Exp Pathol 2006;87:177–84.

Japanese Journal of Clinical Oncology Advance Access published February 27, 2012

JJCO Japanese Journal of Clinical Oncology

Jpn J Clin Oncol 2012
doi:10.1093/jjco/hys012

Original Article

Safety, Efficacy and Pharmacokinetics of Neratinib (HKI-272) in Japanese Patients with Advanced Solid Tumors: A Phase 1 Dose-escalation Study

Yoshinori Ito[1,*], Mitsukuni Suenaga[1], Kiyohiko Hatake[1], Shunji Takahashi[1], Masahiro Yokoyama[1], Yusuke Onozawa[2], Kentaro Yamazaki[2], Shuichi Hironaka[2], Kiyoshi Hashigami[3], Hirotaka Hasegawa[3], Nobuko Takenaka[4] and Narikazu Boku[2]

[1]Department of Medical Oncology, The Cancer Institute of the Japanese Foundation for Cancer Research, Tokyo, [2]Division of Gastrointestinal Oncology, Shizuoka Cancer Center, Shizuoka, [3]Department of Oncology, Clinical R&D, Pfizer Inc, Tokyo and [4]Department of Clinical Pharmacology, Clinical R&D, Pfizer Inc, Tokyo, Japan

*For reprints and all correspondence: Yoshinori Ito, Breast Cancer Division, Department of Medical Oncology, The Cancer Institute of the Japanese Foundation for Cancer Research, 3-8-31 Ariake Koto-ku, Tokyo 135-8550, Japan. E-mail: yito@jfcr.or.jp

Received November 11, 2011; accepted January 26, 2012

Objective: Neratinib (HKI-272), a potent, irreversible, small-molecule, orally administered, pan-ErbB inhibitor that blocks signal transduction via inhibition of three epidermal growth factor receptors [ErbB1, ErbB2 (Her2) and ErbB4], is being developed for the treatment of solid tumors, including breast cancer. This Phase 1 dose-escalation study assessed the safety, tolerability, maximum-tolerated dose, antitumor activity and pharmacokinetics of neratinib in Japanese patients with advanced solid tumors.

Methods: Patients received neratinib 80, 160, 240 or 320 mg orally; each patient enrolled in only one dose cohort. Patients received a single dose in week 1, followed by daily continuous doses. Blood samples collected were on days 1 and 21 for pharmacokinetic analyses.

Results: Twenty-one patients were enrolled (3 breast cancer; 17 colorectal cancer; 1 gastric cancer). Neratinib-related adverse events (all grades) included diarrhea (20 patients), fatigue (14 patients), nausea and abdominal pain (9 patients each) and anorexia (8 patients). Grade $\geq$3 neratinib-related adverse events in two or more patients were diarrhea and anorexia (two patients each). Dose-limiting toxicities were diarrhea and anorexia (two patients, 320 mg dose). The maximum-tolerated dose and recommended dose was neratinib 240 mg once daily. Of 21 evaluable patients, 2 with breast cancer had partial response, 3 had stable disease $\geq$24 weeks, 7 had stable disease $\geq$16 weeks and 9 had progressive disease. Pharmacokinetic analyses indicated that neratinib exposures increased with dose.

Conclusions: The safety, efficacy and pharmacokinetic profiles of neratinib are consistent with those reported for non-Japanese patients and warrant further investigation of neratinib in Japanese patients with solid tumors.

Key words: ErbB2 – maximum-tolerated dose – neratinib – Phase I clinical trial – treatment efficacy

INTRODUCTION

Dysregulation of growth factor signaling due to hyperactivation of the epidermal growth factor receptor (EGFR/ErbB) family of tyrosine kinase receptors has been observed in several cancer types (1) and is associated with increased proliferation, angiogenesis, metastasis and decreased apoptosis (2). Due to its implication in tumorigenesis, inhibition of

this family of kinase receptors may be a novel and viable treatment option for patients who are intolerant to chemotherapy or those refractory to the current standard of care.

Several drugs have been developed and marketed that selectively inhibit the ErbB receptor kinases, such as the small-molecule, reversible, adenosine triphosphate-competitive inhibitors erlotinib and gefitinib, which target ErbB1 (3,4), and lapatinib, which targets both ErbB1 and ErbB2 (Her2) (5). Monoclonal antibodies have also demonstrated antitumor activity, such as trastuzumab, which binds to ErbB2 (6), and panitumumab and cetuximab, which bind to ErbB1 (7,8). There are, however, various limitations to the safety and efficacy of these drugs. For example, gefitinib and erlotinib provide progression-free survival (PFS) times of only 9–13 months in patients with non-small cell lung cancer showing EGFR mutations. Likewise, trastuzumab is associated with response rates of only 15–26% when given as monotherapy (9,10) and 42% in combination with paclitaxel for the treatment of patients with metastatic breast cancer (11). Trastuzumab is also associated with cardiac toxicity, particularly in patients previously treated with anthracyclines (12,13).

Neratinib (HKI-272) is a potent, orally administered, small-molecule, pan-ErbB inhibitor that irreversibly blocks signal transduction via inhibition of ErbB1, ErbB2 and ErbB4 (14–16). Neratinib has shown promising antitumor activity in a variety of solid tumors, including breast cancer and non-small cell lung cancer (17,18). In addition, neratinib can potentially overcome the acquired resistance of the EGFR 'gatekeeper' T790M mutation. This mutation typically develops in the tumors of lung cancer patients that harbor the EGFR kinase domain-sensitizing mutation after treatment with reversible inhibitors such as gefitinib or erlotinib and subsequent disease progression (19–22).

In the Phase 1, first-in-human dose-escalation study of neratinib in patients with solid tumors that was conducted in the USA, the maximum-tolerated dose (MTD) of neratinib was found to be 320 mg once daily (17). In addition, neratinib exposure was dose-dependent and the pharmacokinetic (PK) results favored a once-daily dosing regimen (17). Neratinib was also clinically active in patients with advanced and/or metastatic ErbB2-positive breast cancer, even under conditions of trastuzumab resistance, and was well tolerated as a once-daily orally dosed agent (17). However, due to the primary dose-limiting toxicity (DLT) of diarrhea, the therapeutic dose was limited to 240 mg once daily in later Phase 2 studies. In patients with advanced ErbB2-positive breast cancer, the 16-week PFS rates were 59 and 78% for patients with prior trastuzumab and no prior trastuzumab treatments, respectively, and the objective response rates (ORRs) were 24 and 56%, respectively (18).

Because the efficacy and safety of drugs, such as gefitinib and sunitinib, can vary between Western and Asian populations (23), we assessed the safety and tolerability, and determined the MTD of oral neratinib in Japanese patients with solid tumors in this Phase 1 study. The preliminary antitumor activity and the PK profile of neratinib in the same patient population were also evaluated.

PATIENTS AND METHODS

Study Design

This was a multicenter, open-label, Phase 1, ascending single and multiple oral dose study conducted in Japan to determine the safety, tolerability, MTD, antitumor activity and PK of neratinib in Japanese patients with advanced solid tumors. Each patient participated in only one dose cohort (three to six patients) and received a single dose of neratinib. After a 1-week observation period, patients received neratinib as a continual oral daily dose for up to 6 months (six cycles), or longer at the same dose level if neratinib was well tolerated and the patient showed no evidence of progressive disease (PD).

This study was conducted in accordance with the International Conference on Harmonisation Guideline for Good Clinical Practice and the ethical principles that have origins in the Declaration of Helsinki. The study protocol was approved by an Institutional Review Board and written informed consent was obtained from all patients before their enrollment in this study.

Patient Eligibility

Patients were eligible for enrollment if they were $\geq$20 years of age and had a histologic/cytologic diagnosis of metastatic or advanced cancer that had failed to respond to standard effective therapy or for which no standard effective treatment was available, a life expectancy of $\geq$12 weeks and a measurable lesion as defined by modified Response Evaluation Criteria in Solid Tumors guidelines. Other key inclusion criteria were a performance status of 0–2 on the Eastern Cooperative Oncology Group (ECOG) scale, an absolute neutrophil count of $\geq 1.5 \times 10^9$/l, platelet count $\geq 100 \times 10^9$/l, creatinine level $\leq 1.5\times$ the upper limit of normal and total bilirubin $\leq 1.5\times$ the upper limit of normal.

The main exclusion criteria were the following: anticancer chemotherapy, radiotherapy, immunotherapy or investigational agents within 4 weeks before treatment day 1; prior treatment with anthracyclines with a cumulative dose of doxorubicin or equivalent >400 mg/m^2; automatic electrocardiogram (ECG)-corrected QT (QTc) interval reading at screening >470 ms; left ventricular ejection fraction (LVEF) below the institutional range of normal as measured by echocardiogram; significant gastrointestinal disorders with diarrhea as a major symptom; and a history of clinically significant cardiac disease, including congestive heart failure, myocardial infarction and significant arrhythmia.

Dose Escalation

Neratinib was administered orally once daily with food, preferably in the morning. After administration of the single dose and a 1-week observation period, patients were treated at the same dose level with continual oral daily doses in 28-day cycles. Dose cohorts consisted of neratinib 80, 160, 240 and 320 mg. The starting dose was based on the results

of the Phase 1, first-in-human study of neratinib in patients with solid tumors that was conducted in the USA, in which neratinib-related Grade 3 adverse events (AEs) were not reported at doses $\leq$80 mg (17). The decision to proceed to the next dose level was made after the last patient in a cohort had been evaluated through ~14 days of continuous daily administration. Enrollment at the next dose level occurred according to the following criteria: if no patients experienced a DLT, then three–six patients were enrolled at the next dose level; if one patient experienced a DLT, then an additional six patients were treated at the same dose level and the dose escalated if no more than one of those patients had a DLT. If two or more patients at a dose level experienced a DLT by day 14 of continuous daily dosing, dose escalation stopped and the previous dose level was considered the MTD. If a patient in any dose cohort had a toxicity that met the definition of DLT, then the patient's dose was reduced by one dose level, and if the patient experienced a second DLT, then the dose was further decreased by one dose level. No more than two dose reductions were allowed for any patient.

A DLT was defined as any neratinib-related non-hematologic Grade 3 or any Grade 4 AE according to the National Cancer Institute Common Terminology Criteria for Adverse Events, version 3.0, with the exception of Grade 3 nausea, vomiting, diarrhea or rash, unless the patient was receiving appropriate medical therapy. Additional DLTs included Grade 2 or 3 diarrhea lasting >2 days, for which the patient was receiving appropriate medical therapy or for that which was associated with fever or dehydration. DLTs were assessed during the first 21 days following the administration of the first dose in the continual single-dose period.

Evaluation of Patients

Safety evaluations were based on the incidence and severity of AEs, the DLTs at each dose level and changes in clinical laboratory test results over time. AEs were monitored and recorded continuously during the study, while laboratory evaluations were conducted at screening; on day 1 of the single-dose period; on days 1, 7, 14 and 21 of cycle 1 of the continuous dosing period; on days 1 and 14 of cycles 2 through 6; and at the final evaluation (30 days after the last dose). Other safety assessments included vital signs, interim history, radiographs, cardiac evaluations, echocardiogram and ECGs. The efficacy population included all patients who received $\geq$2 weeks of neratinib therapy and underwent $\geq$1 tumor assessment ~8 weeks after starting continual daily neratinib administration. In addition, patients with disease progression prior to receiving 14 days of neratinib therapy were considered evaluable for efficacy.

PK Analyses

Timed blood samples for PK analyses of neratinib were collected on day 1 and on day 14 (study day 21) of continual daily dose administration. Samples were collected at 0 h (pre-dose) and at 1, 2, 4, 6, 8 and 24 h after dose administration. Samples were also collected at 48 h after dose administration on day 1 of the single-dose period. Plasma neratinib concentrations were measured using a validated liquid chromatography/tandem mass spectrometry method. PK analyses were performed for each patient using non-compartmental methods (24) with WinNonLin® Enterprise application, version 5.1 (Pharsight Corporation, CA, USA). The parameters determined included the following: observed maximum concentration (C_{max}), area under the concentration–time curve (AUC) from time zero extrapolated to infinite time ($AUC_{0-\infty}$), AUC at steady state (AUC_{ss}), AUC from time 0–24 h (AUC_{0-24h}), time of maximum concentration (t_{max}), terminal-phase elimination half-life ($t_{1/2}$), the apparent volume of distribution for the terminal disposition phase (V_z/F) and the apparent oral clearance (CL/F).

The preliminary assessment of dose proportionality was evaluated by the following power model:

$$C_{max}, \quad AUC_{0-\infty} \quad \text{or} \quad AUC_{ss} = \alpha \times dose^{\beta} \qquad (1)$$

where α is the coefficient and β is the exponent of the linear-regression model on log-transformed parameters, C_{max}, $AUC_{0-\infty}$, AUC_{ss} and dose. The 95% confidence intervals (CIs) for the exponents were also calculated. The validity of the power model was evaluated by performing a lack-of-fit test. A P-value for the lack-of-fit test of <0.05 would imply that there was a significant lack of fit in the power model and that the point estimate derived from the power model was not valid.

Determination of Sample Size

Approximately 28 patients were to be enrolled in this study. This estimate was based on a maximum of 6 patients per dose cohort over approximately four dose levels and enrolling 4–7 additional patients (total 10 patients) at the recommended dose. The actual number of patients enrolled was dependent on the tolerability of neratinib and the number of dose levels required to attain the MTD.

The sample size for this study was determined by clinical rather than statistical considerations. With cohort sizes of three to six patients, if the true underlying rates of DLT were 0.1, 0.2, 0.3, 0.4 and 0.5, there would be 0.91, 0.71, 0.49, 0.31 and 0.17 chances, respectively, of escalating to the next higher dose level. If the frequencies of AEs of Grade $\geq$3 were 0.1, 0.25 and 0.5, the probabilities of detecting one or more such events in six patients receiving neratinib would be 0.469, 0.822 and 0.984, respectively, and the probabilities of detecting one or more such events in 10 patients would be 0.651, 0.944 and 0.999, respectively.

Table 1. Patients' demographics and baseline characteristics

Characteristic	Dose cohorts, mg neratinib				
	80 ($n = 3$)	160 ($n = 3$)	240 ($n = 10$)	320 ($n = 5$)	Total ($n = 21$)
Median age, years (range)	54 (44–63)	47 (44–54)	64.5 (39–78)	61 (47–66)	61 (39–78)
Primary diagnosis, *n* (%)					
Breast cancer	0	1	1	1	3 (14)
Colorectal cancer	3	1	9	4	17 (81)
Gastric cancer	0	1	0	0	1 (5)
ECOG performance status, *n* (%)					
0	3	3	9	4	19 (91)
1	0	0	1	1	2 (10)
Prior chemotherapy, immunotherapy or hormonal therapy, *n* (%)					
Yes	3	3	10	5	21 (100)
Prior chemotherapy, *n* (%)					
2	2	1	4	1	8 (38)
3	0	0	2	2	4 (19)
4	0	0	2	1	3 (14)
5	0	1	0	0	1 (5)
6	1	0	1	1	3 (14)
9	0	0	1	0	1 (5)
12	0	1	0	0	1 (5)
Prior radiotherapy, *n* (%)					
Yes	0	1	3	0	4 (19)
No	3	2	7	5	17 (81)
Prior surgical therapy/cancer biopsy, *n* (%)					
Yes	3	3	10	5	21 (100)

ECOG, Eastern Cooperative Oncology Group.

RESULTS

Patient Characteristics

A total of 21 patients (median age: 61 years; range: 39–78 years) were enrolled in this study from March 2007 to March 2009. The baseline characteristics of the 21 patients are presented in Table 1. Seventeen patients had a primary diagnosis of colorectal cancer, three had a diagnosis of breast cancer and one had a diagnosis of gastric cancer. All 21 (100%) patients had an ECOG performance status of 0 or 1. All patients had received prior cancer-related surgery and chemotherapy and four had received prior radiotherapy.

Dose Escalation of Neratinib

Diarrhea and anorexia were the only reported DLTs for two (40%) patients in the 320 mg dose cohort in this study; one patient had Grade 3 diarrhea and Grade 3 anorexia, and the other patient had Grade 2 diarrhea and Grade 3 anorexia. Neratinib 240 mg was determined to be the MTD and was thus used for the expanded MTD cohort. Therefore, the 240 mg cohort was expanded to include an additional seven patients to confirm the safety and tolerability of the MTD of neratinib.

Safety

All 21 (100%) patients completed the single-dose period and then started the continual daily dose period. The median duration of treatment in the continual daily dose period was 14.9 weeks (range: 2.1–39.9 weeks). The median relative dose intensity was 1.00 for each dose level (range in 240 mg: 0.75–1.00), indicating that patients received close to the initial scheduled daily dose.

All 21 patients experienced AEs that were considered neratinib-related (Table 2). The most common neratinib-related AEs were: diarrhea (20 patients, 95%); fatigue (14, 67%); nausea and abdominal pain (9, 43%

Table 2. Neratinib-related adverse events of all grades that occurred in ≥15% of patients and of Grade ≥3 that occurred in one or more patients from screening visit until 30 days after last dose of neratinib

Adverse event	Dose cohorts, mg neratinib				
	80 ($n = 3$)	160 ($n = 3$)	240 ($n = 10$)	320 ($n = 5$)	Total ($n = 21$)
Diarrhea	2	3	10	5	20 (95)
Grade ≥3	0	1	0	1	2 (10)
Fatigue	1	3	6	4	14 (67)
Abdominal pain	1	2	4	2	9 (43)
Nausea	0	3	3	3	9 (43)
Anorexia	0	1	5	2	8 (38)
Grade ≥3	0	0	0	2	2 (10)
Aspartate aminotransferase increased	1	1	4	2	8 (38)
Grade ≥3	0	0	1	0	1 (5)
Blood alkaline phosphatase increased	0	1	6	1	8 (38)
Hemoglobin decreased	0	1	4	3	8 (38)
Alanine aminotransferase increased	1	0	4	2	7 (33)
Grade ≥3	0	0	1	0	1 (5)
Blood albumin decreased	2	1	2	2	7 (33)
Weight decreased	0	1	3	3	7 (33)
Blood triglycerides increased	1	2	2	1	6 (29)
Rash	2	0	3	1	6 (29)
Blood creatine phosphokinase increased	0	0	2	3	5 (24)
Hyperglycemia	1	0	3	1	5 (24)
Pyrexia	0	0	3	2	5 (24)
Vomiting	0	1	3	1	5 (24)
Blood creatinine increased	0	1	1	2	4 (19)
Stomatitis	1	0	2	1	4 (19)
Neutropenia	0	1	0	1	2 (10)
Grade ≥3	0	0	0	1	1 (5)
Esophageal varices	0	0	1	0	1 (5)
Grade ≥3	0	0	1	0	1 (5)

each); increased aspartate aminotransferase levels, increased blood alkaline phosphatase levels, decreased hemoglobin levels and anorexia (8, 38% each); and increased alanine aminotransferase levels, decreased blood albumin levels and decreased weight (7, 33% each). Anorexia and diarrhea were the most common Grade ≥3 neratinib-related AEs (2, 10% each; Table 2). The median onset of diarrhea was 10.0 days and the median duration was 2.0 days. Even though all diarrhea AEs were considered neratinib-related, no patient had a Grade ≥4 event. Diarrhea was managed by dose interruption, dose reduction and appropriate medication and resolved in 90% of the patients. Cardiovascular AEs were reported for one patient who had an LVEF that decreased from normal at baseline to <50%. However, the decrease in LVEF was related to the patient's underlying disease of sinus bradycardia and was considered not related to neratinib therapy by the treating investigator.

Serious AEs were reported for six patients; anorexia and fatigue (two patients each); hydronephrosis, nausea, dysphagia, esophageal varices and dyspnea (one patient each). One neratinib-related serious AE, esophageal varices, was reported for a patient in the 240 mg cohort. No patient discontinued treatment and was withdrawn from this study due to an AE, and no deaths were reported during the study or within 30 days after the last dose was administered.

A total of three (14%) patients had dose reductions due to AEs; two patients in the 320 mg cohort had diarrhea and anorexia, and one patient in the 240 mg cohort had diarrhea. All AEs that led to dose reductions were considered neratinib-related.

Table 3. Best overall response in the evaluable population

Response	Dose cohorts, mg neratinib				
	80 ($n = 3$)	160 ($n = 3$)	240 ($n = 10$)	320 ($n = 5$)	Total ($n = 21$)
CR, *n*	0	0	0	0	0
PR, *n*	0	0	1	1	2
ORR, %	0	0	10.0	20.0	9.5
SD, *n*					
≥16 weeks	1	1	4	1	7
≥24 weeks	0	0	2	1	3
CBR, %	0	0	30.0	40.0	23.8
PD, *n*	2	2	3	2	9

CR, complete response; PR, partial response; ORR, objective response rate (CR + PR); SD, stable disease; CBR, clinical benefit rate (CR + PR + SD ≥24 weeks); PD, progressive disease.

Antitumor Activity

All 21 patients were considered evaluable for efficacy (Table 3). Two of the three patients with primary diagnoses of breast cancer had a partial response (PR). ErbB2 status was positive for one of these two patients but unknown for the other patient; both patients had received a prior trastuzumab-containing regimen. Three patients had stable disease (SD) ≥24 weeks, seven patients had SD ≥16 weeks and nine patients had PD. The ORR [complete response (CR) + PR] for all patients was 9.5% (95% CI: 1.2–30.4)

Table 4. Pharmacokinetic parameters of neratinib in Japanese patients with advanced solid tumors

Dose cohort, mg (*n*)	Parameter, mean (CV%)						
	C_{max} (ng/ml)	t_{max}[a] (h)	$t_{1/2}$ (h)	AUC[b] (ng×h/ml)	CL/F (l/h/kg)	V_z/F (l/kg)	*R*
Study day 1							
80 (3)	33.3 (43)	4.0 (2.0–8.0)	NC	NC	NC	NC	NA
160 (3)	51.4 (43)	3.9 (3.9–4.0)	11.1 (28)	638 (66)	5.8 (61)	84 (45)	NA
240 (10)	76.3 (41)	5.9 (2.0–8.0)	14.3 (19)[c]	1640 (48)[c]	3.7 (97)[c]	65 (63)[c]	NA
320 (5)	93.2 (40)	4.0 (3.9–7.9)	16.0 (13)	2290 (46)	3.0 (61)	71 (69)	NA
Study day 21							
80 (3)	41.9 (62)	4.0 (2.0–6.0)	17.6 (50)	581 (46)	2.7 (35)	76 (81)	1.5 (49)[d]
160 (3)	57.4 (80)	3.9 (2.0–4.0)	12.7 (27)	688 (79)	12.0 (129)	192 (122)	1.3 (60)
240 (10)	81.5 (56)	4.0 (2.0-7.9)	22.7 (88)[e]	1110 (59)[e]	5.4 (74)[e]	149 (74)[e]	1.2 (43)[e]
320 (3)	143.0 (34)	3.9 (0.0-5.9)	22.1 (12)[d]	2040 (10)[d]	2.5 (6)[d]	80 (18)[d]	1.3 (4)[d]

CV%, percent coefficient of variation; C_{max}, peak concentration; t_{max}, time to peak concentration; $t_{1/2}$, terminal phase elimination half-life; AUC, area under the concentration–time curve; CL/F, apparent oral dose clearance; V_z/F, apparent volume of distribution; *R*, accumulation ratio (quotient of AUC_{ss} on day 1 to AUC_{0-24h} on study day 21); NC, not calculated; NA, not applicable.
[a]t_{max} reported as median (range: minimum–maximum).
[b]Reported as AUC from time zero extrapolated to infinite time ($AUC_{0-\infty}$) for study day 1, and the steady-state AUC (AUC_{ss}) for study day 21.
[c]$n = 8$.
[d]$n = 2$.
[e]$n = 9$.

and the clinical benefit rate (CR + PR + SD ≥24 weeks) was 23.8% (95% CI: 8.2–47.2). Durations of response for the two patients with PR were 16.1 and 32.3 weeks, respectively. The median duration of SD was 16.7 weeks (95% CI: 16.3–24.1) among 10 patients with SD. The median time to progression was 16.1 weeks (95% CI: 8.4–17.0) for all patients.

Pharmacokinetics

Plasma samples for PK analyses were available for all 21 patients who received neratinib doses ranging from 80 to 320 mg. Samples collected within 5 days after dose reduction were not included in the PK analysis. The PK parameters are summarized in Table 4. Following single doses of neratinib from 80 to 320 mg on study day 1, the absorption of neratinib was relatively slow with a median t_{max} of 4–6 h and mean $t_{1/2}$ for the 160–320 mg dose cohorts ranged from 11 to 16 h (percent coefficient of variation, 13–28%). Multiple-dose exposure was 1.2- to 1.5-fold greater than single-dose exposure across the entire dose range, as assessed by the mean accumulation ratio (*R*, AUC_{ss} on study day 21 to AUC_{0-24h} on study day 1; Table 4). These results suggest that there is no major accumulation of neratinib after repeated daily administration to patients with solid tumors.

After single and multiple oral doses of neratinib, C_{max}, $AUC_{0-\infty}$ and AUC_{ss} appeared to increase with the increasing dose (Fig. 1). The power-model assessment confirmed the dose proportionality of neratinib administration. For day 1, exponents for C_{max} and $AUC_{0-\infty}$ were 0.73 and 1.28, respectively, and the corresponding 95% CIs of the exponents were 0.23–1.24 and 0.32–2.24. For day 21, the exponents for C_{max} and AUC_{ss} were 0.88 and 0.78, respectively, and the corresponding 95% CIs of the exponents were 0.03–1.73 and −0.17–1.73. For all of the parameters on days 1 and 21, the CIs contained one, suggesting that there is no lack of dose proportionality. In addition, the lack-of-fit tests for the models were not statistically significant, thus suggesting a linear relationship for C_{max}, $AUC_{0-\infty}$ and AUC_{ss} versus dose.

A comparison of our PK results in our Japanese patients versus patients in the neratinib study that was conducted in the USA (17), using our in-house data, is presented in Fig. 2. Although the variability in C_{max}, $AUC_{0-\infty}$ and AUC_{ss} is large, there is overlap of the PK exposures between the Japanese and US studies. This comparison suggests that there are no relevant differences in the PK between Japanese patients and those patients (92% white) in the US study.

DISCUSSION

In this Phase 1 study, neratinib as a single agent was administered to Japanese patients with advanced solid tumors. The reported DLTs were Grades 2 and 3 diarrhea and Grade 3 anorexia for two patients in the 320 mg dose cohorts; therefore, the MTD of neratinib for Japanese patients was determined to be 240 mg once daily. In comparison, the MTD was found to be 320 mg once daily in the Phase 1

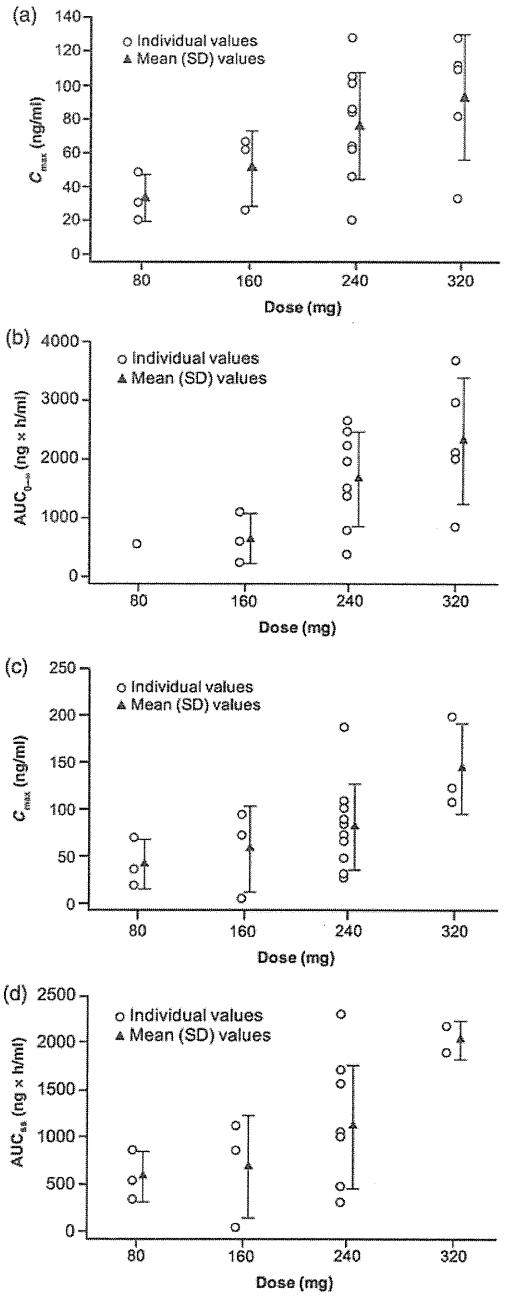

Figure 1. Individual and mean (SD) plasma neratinib exposures versus dose on study day 1 (a) C_{max} versus dose and (b) $AUC_{0-\infty}$ versus dose, and study day 21 (c) C_{max} versus dose and (d) $AUC_{0-\infty}$ versus dose. Patients with advanced solid tumors received single ascending oral doses of neratinib once daily. SD, standard deviation; C_{max}, peak concentration; $AUC_{0-\infty}$, area under the concentration–time curve from time zero extrapolated to infinite time.

study of neratinib that was conducted in the USA in 72 patients (92% white, 6% black or Hispanic, 1% Asian and 1% Middle Eastern) with advanced solid tumors; the DLT was Grade 3 diarrhea [1 (17%) patient in the neratinib 180 mg dose group and 5 (83%) patients in the 400 mg dose group] (17). However, due to gastrointestinal AEs, the

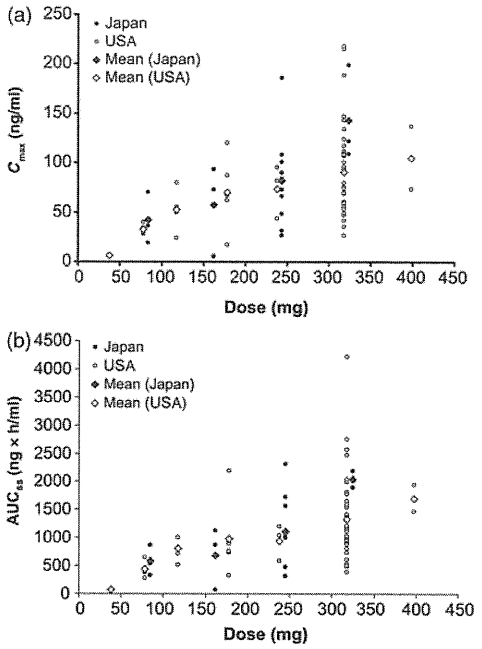

Figure 2. Comparison of neratinib exposures on study day 21: Japan versus US studies. Patients with advanced solid tumors received single ascending oral doses of neratinib once daily; (a) C_{max} versus dose and (b) AUC_{ss} versus dose. C_{max}, peak concentration; AUC_{ss}, area under the concentration–time curve at steady state.

recommended dose in ongoing Phase 3 studies is 240 mg once daily. Although diarrhea was expected in this study and was reported in 20 (95%) patients, no patients were withdrawn from the study or had a serious AE of diarrhea. Diarrhea was managed by dose interruption, dose reduction and appropriate anti-diarrhea medication.

Neratinib demonstrated promising efficacy results in Japanese patients with advanced solid tumors: PR was observed in two (10%) patients with breast cancer; three (14%) patients had SD $\geq$24 weeks and seven (33%) patients had SD $\geq$16 weeks.

PK analyses revealed that after single and multiple oral doses of neratinib, exposures (C_{max}, $AUC_{0-\infty}$ and AUC_{ss}) increased in a dose-dependent manner from 80 to 320 mg. Multiple-dose exposures were 1.2- to 1.5-fold greater than single-dose exposures across the entire dose range, thus suggesting that there was no major accumulation of neratinib after repeated daily administration of neratinib in cancer patients. The mean elimination $t_{1/2}$ on day 1 at the recommended dose of 240 mg was 14.3 h and supports a once-daily dosing regimen. Our PK data are also consistent with that reported for the US Phase 1 study of neratinib and suggest that there are no relevant differences in the PK profiles between Japanese and white patients with cancer.

This study investigated doses of neratinib from 80 to 320 mg daily. The starting dose was chosen based on information from Phase 1 study conducted in the USA (17). In the US study, diarrhea was the main DLT, with five patients in the 400 mg cohort reporting Grade 3 diarrhea. The MTD

in the US study was, therefore, established as 320 mg. In the US study, neratinib-related Grade 3 AEs were not reported at doses $\leq$80 mg. Therefore, a starting dose level of 80 mg was chosen for the current study. Based on the results of pre-clinical toxicity studies, this starting dose (80 mg/body = 48 mg/m^2 based on 1.65 m^2 human body surface area) is one-fifth of the highest non-severely toxic dosage of 45 mg/kg/day (266 mg/m^2/day, with conversion factor of 5.9), which was the highest dose used in a 4-week rat study (data on file). This dose did not elicit severe or life-threatening toxicity. This clinical dose is also supported by dosages [up to 6 mg/kg/day or 107 mg/m^2 (conversion factor of 17.9)] that did not elicit severe or life-threatening toxicity in a 4-week study in dogs (data on file).

The mean steady-state exposure of the doses at which two patients achieved PR were above the minimum efficacious dose exposure (431 ng$\times$h/ml) in nude mice. In addition, the mean steady-state exposure at the therapeutic dose of 240 mg was ~2.6-fold higher than the minimum efficacious dose exposure. However, there was no clear correlation between the dose or exposure and the severity of major AEs (i.e. diarrhea, fatigue, nausea or abdominal pain) because of the small number of patients in this study.

Irreversible inhibition of the EGFR kinase is desirable because such inhibition can occur in the presence of ATP within the cell and can only be overcome by new synthesis of EGFR. Several ATP-competitive EGFR tyrosine kinase inhibitors have been developed and investigated in clinical trials for the treatment of cancer. First-generation irreversible inhibitors include agents such as pelitinib (EKB-569). A US Phase I study showed no major antitumor responses at the MTD of pelitinib (25), although two patients in a Japanese Phase 1 study with advanced non-small cell lung cancer with EGFR mutations and acquired gefitinib resistance showed radiographic tumor regression (26). However, as pelitinib showed limited activity in Her2-dependent tumor models, the development of irreversible inhibitors with improved activity toward Her2-expressing tumors continued (16). It was discovered that attaching a large lipophilic group to the molecule resulted in improved potency for Her2 kinase inhibition (16). Thus, the structure of the second-generation irreversible pan-Her inhibitor neratinib is similar to the structure of pelitinib, but with this different aniline headpiece. The binding model for neratinib at the ATP site of Her2 indicates that the aniline portion of the molecule fits into a long lipophilic pocket. The nature and placement of these groups most likely gives neratinib its improved Her2 activity compared with pelitinib.

In conclusion, the MTD of oral neratinib was determined to be 240 mg once daily in Japanese patients with advanced solid tumors. Neratinib 240 mg was safe and well tolerated, and demonstrated encouraging antitumor activity in this patient population. We therefore recommend that this dose is used for subsequent studies in Japanese patients. The results of this Phase 1 study are consistent with those observed in white patients and warrant further investigation of neratinib in Japanese patients with solid tumors.

Acknowledgements

We thank all the patients who participated in this study. Editorial/medical writing support was provided by Joseph Ramcharan, PhD, at On Assignment Clinical Research, and Kimberly Brooks, PhD, at a MedErgy HealthGroup company, and was funded by Pfizer Inc.

Funding

This work was supported by Wyeth Research, which was acquired by Pfizer Inc in October 2009 [Study 3144A1-104 (ClinicalTrials.gov Identifier: NCT00397046)].

Conflict of interest statement

Yoshinori Ito is a member of the Scientific Advisory Board for Pfizer Inc and has received research support from Bristol-Myers Squibb, Chugai, Novartis, and Wyeth Research (now Pfizer Inc). Masahiro Yokoyama is a consultant for Chugai. Kentaro Yamazaki has received contract research support from Amgen, Chugai, Daiichi-Sankyo, Taiho and Yakult. Kiyoshi Hashigami and Nobuko Takenaka are employees of Pfizer Inc; Hirotaka Hasegawa is a former employee of Pfizer Inc. Narikazu Boku has received research support from Taiho and has received honoraria from Daiichi-Sankyo, Ono, Taiho and Takeda.

References

1. Plowman GD, Culouscou JM, Whitney GS, Green JM, Carlton GW, Foy L, et al. Ligand-specific activation of HER4/p180erbB4, a fourth member of the epidermal growth factor receptor family. *Proc Natl Acad Sci USA* 1993;90:1746–50.
2. Ciardiello F, De Vita F, Orditura M, Tortora G. The role of EGFR inhibitors in nonsmall cell lung cancer. *Curr Opin Oncol* 2004;16:130–5.
3. Cohen MH, Johnson JR, Chen YF, Sridhara R, Pazdur R. FDA drug approval summary: erlotinib (Tarceva) tablets. *Oncologist* 2005;10:461–6.
4. Cohen MH, Williams GA, Sridhara R, Chen G, Pazdur R. FDA drug approval summary: gefitinib (ZD1839) (Iressa) tablets. *Oncologist* 2003;8:303–6.
5. Xia W, Mullin RJ, Keith BR, Liu LH, Ma H, Rusnak DW, et al. Anti-tumor activity of GW572016: a dual tyrosine kinase inhibitor blocks EGF activation of EGFR/erbB2 and downstream Erk1/2 and AKT pathways. *Oncogene* 2002;21:6255–63.
6. Carter P, Presta L, Gorman CM, Ridgway JB, Henner D, Wong WL, et al. Humanization of an anti-p185HER2 antibody for human cancer therapy. *Proc Natl Acad Sci USA* 1992;89:4285–9.
7. Yang XD, Jia XC, Corvalan JR, Wang P, Davis CG. Development of ABX-EGF, a fully human anti-EGF receptor monoclonal antibody, for cancer therapy. *Crit Rev Oncol Hematol* 2001;38:17–23.
8. Baselga J. The EGFR as a target for anticancer therapy—focus on cetuximab. *Eur J Cancer* 2001;37(Suppl 4):S16–22.
9. Cobleigh MA, Vogel CL, Tripathy D, Robert NJ, Scholl S, Fehrenbacher L, et al. Multinational study of the efficacy and safety of humanized anti-HER2 monoclonal antibody in women who have

HER2-overexpressing metastatic breast cancer that has progressed after chemotherapy for metastatic disease. *J Clin Oncol* 1999;17:2639–48.
10. Vogel CL, Cobleigh MA, Tripathy D, Gutheil JC, Harris LN, Fehrenbacher L, et al. Efficacy and safety of trastuzumab as a single agent in first-line treatment of HER2-overexpressing metastatic breast cancer. *J Clin Oncol* 2002;20:719–26.
11. Seidman AD, Berry D, Cirrincione C, Harris L, Muss H, Marcom PK, et al. Randomized phase III trial of weekly compared with every-3-weeks paclitaxel for metastatic breast cancer, with trastuzumab for all HER-2 overexpressors and random assignment to trastuzumab or not in HER-2 nonoverexpressors: final results of Cancer and Leukemia Group B protocol 9840. *J Clin Oncol* 2008;26:1642–9.
12. Slamon DJ, Leyland-Jones B, Shak S, Fuchs H, Paton V, Bajamonde A, et al. Use of chemotherapy plus a monoclonal antibody against HER2 for metastatic breast cancer that overexpresses HER2. *N Engl J Med* 2001;344:783–92.
13. Seidman A, Hudis C, Pierri MK, Shak S, Paton V, Ashby M, et al. Cardiac dysfunction in the trastuzumab clinical trials experience. *J Clin Oncol* 2002;20:1215–21.
14. Rabindran SK, Discafani CM, Rosfjord EC, Baxter M, Floyd MB, Golas J, et al. Antitumor activity of HKI-272, an orally active, irreversible inhibitor of the HER-2 tyrosine kinase. *Cancer Res* 2004;64:3958–65.
15. Rabindran SK. Antitumor activity of HER-2 inhibitors. *Cancer Lett* 2005;227:9–23.
16. Tsou HR, Overbeek-Klumpers EG, Hallett WA, Reich MF, Floyd MB, Johnson BD, et al. Optimization of 6,7-disubstituted-4-(arylamino)quinoline-3-carbonitriles as orally active, irreversible inhibitors of human epidermal growth factor receptor-2 kinase activity. *J Med Chem* 2005;48:1107–31.
17. Wong KK, Fracasso PM, Bukowski RM, Lynch TJ, Munster PN, Shapiro GI, et al. A phase I study with neratinib (HKI-272), an irreversible pan ErbB receptor tyrosine kinase inhibitor, in patients with solid tumors. *Clin Cancer Res* 2009;15:2552–8.
18. Burstein HJ, Sun Y, Dirix LY, Jiang Z, Paridaens R, Tan AR, et al. Neratinib, an irreversible ErbB receptor tyrosine kinase inhibitor, in patients with advanced ErbB2-positive breast cancer. *J Clin Oncol* 2010;28:1301–7.
19. Kwak EL, Sordella R, Bell DW, Godin-Heymann N, Okimoto RA, Brannigan BW, et al. Irreversible inhibitors of the EGF receptor may circumvent acquired resistance to gefitinib. *Proc Natl Acad Sci USA* 2005;102:7665–70.
20. Ji H, Li D, Chen L, Shimamura T, Kobayashi S, McNamara K, et al. The impact of human EGFR kinase domain mutations on lung tumorigenesis and *in vivo* sensitivity to EGFR-targeted therapies. *Cancer Cell* 2006;9:485–95.
21. Ji H, Zhao X, Yuza Y, Shimamura T, Li D, Protopopov A, et al. Epidermal growth factor receptor variant III mutations in lung tumorigenesis and sensitivity to tyrosine kinase inhibitors. *Proc Natl Acad Sci USA* 2006;103:7817–22.
22. Shimamura T, Ji H, Minami Y, Thomas RK, Lowell AM, Shah K, et al. Non-small-cell lung cancer and Ba/F3 transformed cells harboring the ERBB2 G776insV_G/C mutation are sensitive to the dual-specific epidermal growth factor receptor and ERBB2 inhibitor HKI-272. *Cancer Res* 2006;66:6487–91.
23. Iwasaki M, Hinotsu S, Katsura J. Clinical trials and approval of anti-cancer agents. *Jpn J Clin Oncol* 2010;40(Suppl 1):i65–9.
24. Evans WE, Schentag JJ, Jusko WJ. *Applied Pharmacokinetics: Principles of Therapeutic Drug Monitoring*. Vancouver: Lippincott Williams & Wilkins 1992.
25. Erlichman C, Hidalgo M, Boni JP, Martins P, Quinn SE, Zacharchuk C, et al. Phase I study of EKB-569, an irreversible inhibitor of the epidermal growth factor receptor, in patients with advanced solid tumors. *J Clin Oncol* 2006;24:2252–60.
26. Yoshimura N, Kudoh S, Kimura T, Mitsuoka S, Matsuura K, Hirata K, et al. EKB-569, a new irreversible epidermal growth factor receptor tyrosine kinase inhibitor, with clinical activity in patients with non-small cell lung cancer with acquired resistance to gefitinib. *Lung Cancer* 2006;51:363–8.

Cancer Science
The official journal of the Japanese Cancer Association JCA

Phase I study of anti-CD22 immunoconjugate inotuzumab ozogamicin plus rituximab in relapsed/refractory B-cell non-Hodgkin lymphoma

Michinori Ogura,[1,7] Kiyohiko Hatake,[2] Kiyoshi Ando,[3] Kensei Tobinai,[4] Kota Tokushige,[5] Chiho Ono,[5] Taro Ishibashi[5] and Erik Vandendries[6]

[1]Department of Hematology and Oncology, Nagoya Daini Red Cross Hospital, Nagoya; [2]Division of Medical Oncology and Hematology, Cancer Institute Hospital, Tokyo; [3]Division of Hematology/Oncology, Department of Internal Medicine, Tokai University Hospital, Isehara; [4]Hematology and Stem Cell Transplantation Division, National Cancer Center Hospital, Tokyo; [5]Clinical Research, Pfizer Japan Inc, Tokyo, Japan; [6]Pfizer Inc, Cambridge, Massachusetts, USA

(Received November 10, 2011/Revised January 31, 2012/Accepted February 6, 2012/Accepted manuscript online February 15, 2012/Article first published online March 20, 2012)

Inotuzumab ozogamicin (CMC-544), a humanized anti-CD22 antibody conjugated to the potent cytotoxic antibiotic calicheamicin, targets the CD22 antigen expressed on the majority of B-cell non-Hodgkin lymphomas. This phase I study assessed the tolerability, safety, pharmacokinetics, and preliminary efficacy of inotuzumab ozogamicin administered intravenously in combination with rituximab in Japanese patients with relapsed or refractory B-cell non-Hodgkin lymphoma. Ten patients were administered rituximab 375 mg/m^2 followed by inotuzumab ozogamicin at the maximum tolerated dose (1.8 mg/m^2). Treatment was repeated every 28 days up to eight cycles, or until occurrence of disease progression or intolerable toxicity. The safety profile was similar to that of inotuzumab ozogamicin monotherapy, with hematologic adverse events occurring most frequently. The most common grade three or higher adverse events were thrombocytopenia (70%), neutropenia (50%), leukopenia (30%), and lymphopenia (30%). The overall response rate was 80% (8/10; 95% CI, 44–98%). Drug exposure increased with successive doses, similar to the pharmacokinetic profiles observed in previous phase I monotherapy studies. Efficacy results suggested promising antitumor activity, and the overall findings support the continued clinical development of this therapeutic regimen in patients with relapsed or refractory B-cell non-Hodgkin lymphoma. This trial was registered at www.ClinicalTrials.gov as NCT00724971. (*Cancer Sci* 2012; 103: 933–938)

CD22, a B-cell antigen expressed on >90% of B-lymphoid malignancies,[1] represents an attractive therapeutic target for treatment of B-cell non-Hodgkin lymphoma (NHL). CD22 is not routinely shed into the extracellular environment;[2] rather, CD22 is rapidly internalized upon binding with a ligand or antibody, allowing efficient delivery of targeted cytotoxic agents.[3] Inotuzumab ozogamicin (CMC-544) is a targeted chemotherapy agent composed of a humanized anti-CD22 antibody conjugated to calicheamicin, a potent cytotoxic antibiotic. *In vitro*, inotuzumab ozogamicin has demonstrated enhanced cytotoxic activity compared with untargeted uptake of calicheamicin.[2] Additionally, CD22 is expressed primarily on mature B-lymphocytes, with limited expression on lymphocyte precursor cells and no expression on memory B cells; therefore, minimal impact of inotuzumab ozogamicin on long-term immune function is expected.

Inotuzumab ozogamicin demonstrated promising cytotoxic activity both as a single agent and in combination with rituximab in xenograft models and *in vitro* studies.[2,4,5] Rituximab, an anti-CD20 monoclonal antibody, is indicated for single-agent use or in combination with chemotherapy for treatment of low-grade or follicular, CD20-positive, B-cell NHL, and in combination with chemotherapy for treatment of diffuse large B-cell, CD20-positive NHL.[6] Although rituximab has been effectively used in combination with chemotherapy for indolent and aggressive B-cell NHLs, some patients are not responsive, while those who do respond often experience relapse.[7] Mechanisms of rituximab resistance may include downregulation of CD20 and increased expression of complement inhibitory proteins.[8] Newer monoclonal antibodies that target B-cell antigens other than CD20 may be effective in rituximab-resistant B-cell NHL or work in synergistic fashion with rituximab to improve B-cell NHL treatment efficacy.[9] As both CD22 and CD20 are expressed in most patients with B-cell NHL,[1,7] inotuzumab ozogamicin and rituximab combination therapy in B-cell NHL may enhance the therapeutic advantage of each agent.[5]

Clinical activity was observed with inotuzumab ozogamicin monotherapy at the maximum tolerated dose (MTD) of 1.8 mg/m^2 i.v. every 28 days.[10,11] Results of inotuzumab ozogamicin at the MTD in combination with rituximab in non-Japanese patients with relapsed or refractory B-cell NHL has shown promising efficacy with a safety profile similar to that reported for inotuzumab ozogamicin alone.[12] The current study assessed the tolerability and initial safety profile of inotuzumab ozogamicin plus rituximab in Japanese patients with relapsed or refractory B-cell NHL. Secondary objectives included evaluating the pharmacokinetics and preliminary efficacy of this drug combination.

Materials and Methods

Patients. Eligible patients were aged 20–74 years, with a diagnosis of CD20- and CD22-positive B-cell NHL according to the World Health Organization classification.[13] The disease must have progressed after one or two prior therapies, and prior treatment must have included one or more doses of rituximab therapy (monotherapy or combined with chemotherapy). Maintenance therapy with rituximab was considered part of the preceding induction regimen, and patients could not be refractory to rituximab (i.e. progressive disease [PD] under treatment or <6 months of protocol therapy initiation). Other inclusion criteria included an Eastern Cooperative Oncology Group (ECOG) Performance Status ≤ 1; life expectancy

[7]To whom correspondence should be addressed.
E-mail: mi-ogura@naa.att.ne.jp

doi: 10.1111/j.1349-7006.2012.02241.x

$\geq$12 weeks; adequate organ function (absolute neutrophil count [ANC] $\geq 1.5 \times 10^9$/L and platelet count $\geq 100 \times 10^9$/L; serum creatinine $\leq 1.5 \times$ upper limit of normal [ULN] and urine protein to creatinine ratio of ≤ 0.2; total bilirubin $\leq 1.5 \times$ ULN, aspartate aminotransferase [AST] and alanine aminotransferase [ALT] $\leq 2.5 \times$ ULN); and ≥ 1 measurable lesion $\geq 1.5 \times 1.5$ cm by computed tomography (CT) scan. Patients who had received radioimmunotherapy or prior treatment with anti-CD22 antibodies were excluded. Prior allogeneic hematopoietic stem cell transplant was not allowed, and patients with prior autologous transplant were eligible if it occurred >6 months before the first study dose. No chemotherapy, anti-lymphoma immunosuppressive therapy, growth factors (except erythropoietin), or investigational agents <28 days before the first study dose (<6 weeks for nitrosoureas or mitomycin C) was allowed.

The study was conducted in accordance with the Declaration of Helsinki. All patients provided written informed consent, and the protocol was approved by institutional review board at each site. This trial was registered at www.ClinicalTrials.gov (Identifier: NCT00724971).

Study design. This phase I, open-label, single-arm study evaluated the tolerability, safety, pharmacokinetics, and preliminary efficacy of inotuzumab ozogamicin administered i.v. with rituximab to Japanese patients with B-cell NHL. Screening procedures were performed within 21 days of study treatment initiation and included: medical history and physical examination; ECOG Performance Status; CD20/CD22 immunophenotyping of the B-cell lymphoma; electrocardiogram (ECG) and echocardiogram; complete chemistry panel; complete blood count (CBC) with differential; chest radiograph; CT scans of the chest, abdomen, and pelvis; clinical disease and tumor site assessments; bone marrow aspiration and/or biopsy; urinalysis; and testing for serum antibodies to inotuzumab ozogamicin and rituximab.

A fixed standard dose of rituximab 375 mg/m^2 was administered i.v. on day 1 of a 28-day (±2 days) cycle followed by inotuzumab ozogamicin 1.8 mg/m^2 i.v. on day 2 of the cycle. Treatment was repeated for up to eight cycles or until the occurrence of PD, intolerable toxicity, or patient refusal. Patients were followed for a minimum period of 1 year from the first dosing to assess progression-free survival (PFS). Six patients were to be enrolled in the first cohort; if two or fewer patients experienced a dose-limiting toxicity (DLT) within 28 days after the first dose, the dose and administration schedule would be considered reasonable and an additional four patients would be enrolled in an expanded cohort (10 patients total). If more than two of six patients experienced a DLT in the first 28 days, the tolerability of lower doses of inotuzumab ozogamicin (e.g. 1.3 mg/m^2) would be explored.

A DLT was defined as any of the following that were at least possibly related to study treatment: any grade 3/4 nonhematologic toxicity (except grade 3 nausea or vomiting, unless the patient had received optimal supportive therapy); febrile neutropenia (grade 4 ANC and temperature $\geq$38.0°C); grade 4 ANC ≥ 7 days duration; grade 4 thrombocytopenia ≥ 3 days duration or grade 3/4 thrombocytopenia associated with bleeding tendency requiring platelet transfusion; and delayed recovery (to grade ≤ 1 or baseline, except alopecia) from toxicity related to the study drug that delayed initiation of the next dose by > 2 weeks.

Safety assessment. All patients who received one or more doses of inotuzumab ozogamicin or rituximab were included in the safety analysis (safety population). Safety was monitored through physical examinations, interim history, and laboratory tests. Interim physical examinations, including liver and spleen assessments, occurred every cycle before treatment administration if deemed necessary. Vital signs were measured on each day of inotuzumab ozogamicin administration. Complete chemistry panel and CBC with differential were assessed weekly during the first four cycles and biweekly during the last four cycles. Complete spot urinalysis was performed on day 1 of every other cycle beginning with cycle 2. ECG and chest radiograph were conducted at treatment completion. Adverse events (AEs) were graded using the National Cancer Institute Common Terminology Criteria for Adverse Events, version 3.0. Patients were monitored for AEs for 28–42 days after the last dose of inotuzumab ozogamicin, regardless of causality, and patients with evidence of treatment-related AEs at the end of treatment visit were followed until the AEs resolved or were determined to be irreversible.

Efficacy evaluation. Efficacy analyses were based on the intention-to-treat (ITT) and evaluable populations. The ITT population included all patients who were enrolled into the intended dose scheme, and the evaluable population included all patients who received two or more cycles of the study treatment, had a baseline tumor CT scan, and had undergone one or more post-baseline tumor assessments. Tumor responses were evaluated by investigator's assessment according to the International Response Criteria for NHL.[14] Overall response rate (ORR) was defined as the proportion of patients achieving complete response (CR), unconfirmed complete response (CRu), or partial response (PR). Duration of overall response was defined as the interval between first CR, CRu, or PR, until relapse or PD. PFS was defined as the interval between the first study dose and relapse, PD, or death, censored at the last tumor evaluation date. PFS rate at 1 year, defined as the proportion of patients without an event (relapse, PD, or death), was used as an early determination of PFS. Overall survival (OS) was defined as the interval between the first study dose and death, censored at the last date known alive.

Tumor responses were determined from CT scans, clinical information (e.g. liver and spleen size), "B-symptoms" (e.g. fever, night sweats, and weight loss), laboratory assessments (e.g. bone marrow biopsies), and biochemical markers of disease activity (e.g. lactate dehydrogenase). Tumor sites and clinical disease measurements were assessed: approximately every 8 weeks during treatment (or earlier with clinical evidence of tumor response), at the end of treatment visit, and approximately every 12 weeks during follow-up visits. If clinically indicated, CT scans were performed earlier than scheduled, and a confirmatory assessment was performed within 4 weeks of a documented tumor response. Tumor assessments continued until PD or death occurred, or subsequent anti-lymphoma treatment was administered.

Pharmacokinetic analyses. Serum concentrations of inotuzumab ozogamicin, total calicheamicin, and free (unconjugated) calicheamicin were determined using a validated ELISA.[10] The quantitation ranges for inotuzumab ozogamicin, total calicheamicin, and free calicheamicin were 52.2–1400, 5–100, and 1.25–150 ng/mL, respectively. Timed blood samples for pharmacokinetic analyses were collected from cycles 1 to 3, at 0 (pre-dose), 1 (before the end of infusion), 4, 48, 144, 192, 312, 480, and 648 h relative to the start of inotuzumab ozogamicin infusion; sample collection for pharmacokinetics was not collected beyond cycle 3. Pharmacokinetic parameters of inotuzumab ozogamicin and total calicheamicin were estimated by a non-compartmental method using WinNonlin, version 5.1 (Pharsight, Mountain View, CA, USA). Validated ELISAs were used for the detection of antibodies to inotuzumab ozogamicin and rituximab. The pharmacokinetic profile of rituximab was not evaluated.

Statistics. The safety and antitumor activity of inotuzumab ozogamicin plus rituximab were evaluated on an exploratory basis and summarized using descriptive statistics. Clopper-Pearson methodology was used to estimate the confidence interval

doi: 10.1111/j.1349-7006.2012.02241.x